
Supporting Information

1-D “Platinum Wire” Stacking Structure Built of Platinum(II) Diimine Bis(σ -acetylide) Units with Luminescence in the NIR Region

Jiajia Kang,[†] Xiaoxin Zhang,[†] Huajun Zhou,[‡] Xuqiao Gai,[†] Ting Jia,[†] Liang Xu,[†] Jianjun Zhang,[†] Yanqin Li,[†] and Jun Ni^{*,†}

[†]*College of Chemistry, Dalian University of Technology, Linggong Road No. 2, Dalian 116024, P. R. China,*

[‡]*High Density Electronics Center, University of Arkansas, Fayetteville, Arkansas 72701, United States*

Contents

Table S1. Crystal data and structure refinement for 1 ·DMSO, 1 ·1/2(CH ₃ CN) and 1 ·1/8(CH ₂ Cl ₂).....	5
Table S2. Selected bond lengths (Å), bond angles (°) and the shortest Pt···Pt (Å) distance for 1 ·DMSO, 1 ·1/2(CH ₃ CN) and 1 ·1/8(CH ₂ Cl ₂)	6
Table S3. Hydrogen-bonding geometry (Å, °) and short interactions in 1 ·DMSO, 1 ·1/2(CH ₃ CN) and 1 ·1/8(CH ₂ Cl ₂).....	7
Table S4. Partial molecular orbital compositions (%) in the ground state for 1 in dichloromethane solution from the TD-DFT calculation.....	8
Table S5. Absorption and emission transition properties of 1 in dichloromethane solution by TD-DFT method at the PBE1PBE level with the polarized continuum model (PCM).....	9
Table S6. Partial molecular orbital compositions (%) in the ground state for the two-molecule model of 1 ·DMSO in the solid state by TD-DFT method at the PBE1PBE level.....	11
Table S7. Absorption and emission transition properties for the two-molecule model of 1 ·DMSO in the solid state by TD-DFT method at the PBE1PBE level.....	12
Table S8. Partial molecular orbital compositions (%) in the ground state for the two-molecule model of 1 ·1/2(CH ₃ CN) in the solid state by TD-DFT method at the PBE1PBE level.....	14
Table S9. Absorption and emission transition properties for the two-molecule model of 1 ·1/2(CH ₃ CN) in the solid state by TD-DFT method at the PBE1PBE level.....	15
Table S10. Partial molecular orbital compositions (%) in the ground state for the two-molecule model of 1 ·1/8(CH ₂ Cl ₂) in the solid state by TD-DFT method at the PBE1PBE level.....	16
Table S11. Absorption and emission transition properties for the two-molecule model of 1 ·1/8(CH ₂ Cl ₂) in the solid state by TD-DFT method at the PBE1PBE level.....	17
Table S12. Partial molecular orbital compositions (%) in the ground state for the three-molecule model of 1 ·1/8(CH ₂ Cl ₂) in the solid state by TD-DFT method at the PBE1PBE level.....	19
Table S13. Absorption and emission transition properties for the three-molecule model of 1 ·1/8(CH ₂ Cl ₂) in the solid state by TD-DFT method at the PBE1PBE level.....	20

Table S14. Partial molecular orbital compositions (%) in the ground state for the four-molecule model of 1·1/8(CH₂Cl₂) in the solid state by TD-DFT method at the PBE1PBE level.....	22
Table S15. Absorption and emission transition properties for the four-molecule model of 1·1/8(CH₂Cl₂) in the solid state by TD-DFT method at the PBE1PBE level.....	23
Table S16. Partial molecular orbital compositions (%) in the ground state for the five-molecule model of 1·1/8(CH₂Cl₂) in the solid state by TD-DFT method at the PBE1PBE level.....	25
Table S17. Absorption and emission transition properties for the five-molecule model of 1·1/8(CH₂Cl₂) in the solid state by TD-DFT method at the PBE1PBE level.....	26
Figure S1. The $\pi\text{-}\pi$ stacking interactions within the quasi-dimeric structure of 1·DMSO (a) and dimeric structure of 1·1/2(CH₃CN) (b), and one dimeric unit showing the $\pi\text{-}\pi$ stacking interactions in the 1-D linear chain of 1·1/8(CH₂Cl₂) (c). The hydrogen atoms are omitted for clarity. Symmetry code: a. 2-x, 1-y, 2-z; b. 1-x, -y, -z; c. 1-x, 1-y, 1-z; d. -x, 1-y, 1-z.....	28
Figure S2. The interactions between adjacent dimeric structures in complex 1·1/2(CH₃CN) . The hydrogen atoms not participate in hydrogen bond are omitted for clarity. Symmetry code: a. -x, -y, -z; b. -2+x, -1+y, -1+z.....	29
Figure S3. The hydrogen bonds between solvate molecules and Pt(II) moieties in complex 1·DMSO and 1·1/2(CH₃CN) . The hydrogen atoms not important are omitted for clarity. Symmetry code: a. x, y, 1+z; b. -x, -y, -z; c. -1+x, y, z.....	30
Figure S4. Packing diagrams of 1·DMSO (a) and 1·1/2(CH₃CN) (b), showing the Pt(II) moieties are well separated by the solvent molecules in the two phases.....	31
Figure S5. The stacking diagram of 1·1/8(CH₂Cl₂) , showing the CH ₂ Cl ₂ solvate molecules located in space of crystal lattice.....	32
Figure S6. The Pt···Pt distances and interplanar distances in the stacking structures of 1·DMSO (a), 1·1/2(CH₃CN) (b), and 1·1/8(CH₂Cl₂) (c).....	33
Figure S7. Low-energy absorption (dash lines) and emission spectra (solid lines) of 1 in various solvents at ambient temperature.....	34
Figure S8. Emission spectra of 1 in dichloromethane solution with different concentration.....	35
Figure S9. The excitation spectra of solid samples 1·DMSO , 1·1/2(CH₃CN) , and 1·1/8(CH₂Cl₂) at ambient temperature.....	36

Figure S10. Emission spectral changes of solid 1 ·DMSO in response to CH ₃ CN vapor (left) and 1 ·1/2(CH ₃ CN) to DMSO vapor (right), showing gradual interconversions between two vibronic-structured emission bands (540 and 570 nm) and a broad unstructured emission band (625 nm).....	37
Figure S11. The XRD diagrams recorded in a reversible vapochromic cycle 1 ·DMSO \rightleftharpoons 1 ·1/2(CH ₃ CN), showing dynamic variations of XRD patterns from 1 ·DMSO \rightarrow 1 ·1/2(CH ₃ CN) upon exposure of 1 ·DMSO into a saturated CH ₃ CN vapor, and the XRD patterns from 1 ·1/2(CH ₃ CN) \rightarrow 1 ·DMSO by exposing 1 ·1/2(CH ₃ CN) into DMSO vapor at ambient temperature.....	38
Figure S12. Emission spectral changes (left is in visible region and right is in NIR region) of solid 1 ·1/2(CH ₃ CN) sample in response to CH ₂ Cl ₂ vapor (a) and 1 ·1/8(CH ₂ Cl ₂) in response to CH ₃ CN vapor (b), showing gradual interconversions between emission bands in visible region (625 nm) and in NIR region (1022 nm).....	39
Figure S13. The XRD diagrams recorded in a reversible vapochromic cycle 1 ·1/2(CH ₃ CN) \rightleftharpoons 1 ·1/8(CH ₂ Cl ₂), showing dynamic variations of XRD patterns from 1 ·1/2(CH ₃ CN) \rightarrow 1 ·1/8(CH ₂ Cl ₂) upon exposure of 1 ·1/2(CH ₃ CN) into a saturated CH ₂ Cl ₂ vapor, and the XRD patterns from 1 ·1/8(CH ₂ Cl ₂) \rightarrow 1 ·1/2(CH ₃ CN) by exposing 1 ·1/8(CH ₂ Cl ₂) into CH ₃ CN vapor at ambient temperature.....	40
Figure S14. Thermogravimetric analysis curves of the three heated samples 1a , 1b and 1c	41
Figure S15. Plots of the frontier molecular orbitals involved in the absorption transition for complex 1 in dichloromethane solution (isovalue = 0.02).....	42
Figure S16. Plots of the frontier molecular orbitals involved in the absorption transition for the two-molecule model of 1 ·DMSO (isovalue = 0.02).....	44
Figure S17. Plots of the frontier molecular orbitals involved in the absorption transition for the two-molecule model of 1 ·1/2(CH ₃ CN) (isovalue = 0.02).....	46
Figure S18. Plots of the frontier molecular orbitals involved in the absorption transition for two-molecule model of 1 ·1/8(CH ₂ Cl ₂) (isovalue = 0.02).....	48
Figure S19. Plots of the frontier molecular orbitals involved in the absorption transition for three-molecule model of 1 ·1/8(CH ₂ Cl ₂) (isovalue = 0.02).....	50
Figure S20. Plots of the frontier molecular orbitals involved in the absorption transition for four-molecule model of 1 ·1/8(CH ₂ Cl ₂) (isovalue = 0.02).....	52

Figure S21. Plots of the frontier molecular orbitals involved in the absorption transition for five-molecule model of **1·1/8(CH₂Cl₂)** (isovalue = 0.02).....54

Table S1. Crystal data and structure refinement for **1**·DMSO, **1**·1/2(CH₃CN) and **1**·1/8(CH₂Cl₂).

	1 ·DMSO	1 ·1/2CH ₃ CN	1 ·1/8(CH ₂ Cl ₂)
Empirical formula	C ₃₂ H ₃₀ Br ₂ N ₂ OPtS	C ₆₂ H ₅₁ Br ₄ N ₅ Pt	C ₂₄₁ H ₁₉₄ Br ₁₆ Cl ₂ N ₁₆ Pt ₈
<i>M</i>	845.52	1575.90	6224.30
Crystal system	triclinic	triclinic	monoclinic
Space group	<i>P</i> - <i>I</i>	<i>P</i> - <i>I</i>	<i>C</i> 2/ <i>c</i>
<i>a</i> / Å	10.6084(7)	8.9811(4)	22.200(12)
<i>b</i> / Å	12.8660(8)	15.4169(8)	21.156(12)
<i>c</i> / Å	13.3514(9)	20.7934(11)	13.262(7)
α / °	61.360(4)	99.006(4)	90
β / °	76.813(5)	95.653(3)	96.522(6)
γ / °	83.798(5)	98.947(3)	90
<i>V</i> / Å ³	1557.17(18)	2786.6(2)	6188(6)
<i>Z</i>	2	2	1
<i>D_c</i> / g·cm ⁻³	1.803	1.878	1.670
μ(mm ⁻¹)	7.166	7.927	7.158
Radiation (λ, Å)	0.71073	0.71073	0.71073
<i>T</i> / K	296(2)	296(2)	296(2)
<i>F</i> (000)	816	1508	2970
<i>R_{int}</i>	0.030	0.032	0.039
Reflections collected / uniques	10723/5449	13825/9659	15210/5425
Observed reflections (<i>I</i> >2σ(<i>I</i>))	4645	7222	3077
<i>R</i> 1 ^a (<i>I</i> >2σ(<i>I</i>))	0.0325	0.0540	0.0425
<i>wR</i> 2 ^b (all data)	0.0775	0.1547	0.1319
GOF	1.017	1.029	1.067

^a*R*1 = Σ|*F_o*-*F_c*|/Σ*F_o*, ^b*wR*2 = Σ[w(*F_o*²-*F_c*²)²]/Σ[w(*F_o*²)]^{1/2}

Table S2. Selected bond lengths (Å), bond angles (°) and the shortest Pt···Pt (Å) distance for **1**·DMSO, **1**·1/2(CH₃CN) and **1**·1/8(CH₂Cl₂).

	1 ·DMSO	1 ·1/2(CH ₃ CN)	1 ·1/8(CH ₂ Cl ₂)
Shortest Pt···Pt distance	4.845	4.882	3.341
Pt-N	2.074(5)	2.0633(5)	2.0459(6)
	2.066(4)	2.0482(7)	2.0607(6)
Pt-C	1.946(6)	1.961(10)	1.959(11)
	1.959(7)	1.9055(6)	1.9797(7)
N-Pt-N	78.89(17)	79.02(3)	79.25(3)
C-Pt-N	94.4(2)	94.5(3)	94.5(3)
C-Pt-N	95.9(2)	95.26(3)	97.58(3)
C-Pt-C	90.8(2)	91.9(4)	88.00(3)
			88.9(4)

Table S3. Hydrogen-bonding geometry (\AA , $^\circ$) and short interactions in **1**·DMSO, **1**·1/2(CH₃CN) and **1**·1/8(CH₂Cl₂).

1 ·DMSO					
<i>D</i> -H··· <i>A</i>	<i>D</i> -H	H··· <i>A</i>	<i>D</i> ··· <i>A</i>	<i>D</i> -H··· <i>A</i>	Symmetry code
C4-H4···O1	0.93	2.38	3.249(9)	156	x, y, 1+z
C7-H7···O1	0.93	2.44	3.280(8)	150	x, y, 1+z

	center...center	Symmetry code
$\pi(\text{Cg1})\cdots\pi(\text{C11}\equiv\text{C12})$	3.455	2-x, 1-y, 2-z

Cg1 is the pyridine ring containing N1 atom.

1 ·1/2(CH ₃ CN)					
<i>D</i> -H··· <i>A</i>	<i>D</i> -H	H··· <i>A</i>	<i>D</i> ··· <i>A</i>	<i>D</i> -H··· <i>A</i>	Symmetry code
C02-H02A··· $\pi(\text{C11}\equiv\text{C12})$	0.96	2.76	3.598(14)	146	-
C4-H4···N01	0.93	2.69	3.606	170	-x, -y, -z
C7-H7···N01	0.93	2.60	3.510(10)	167	-x, -y, -z
C20-H20A···Br3	0.96	2.81	3.577(12)	137	2-x, 1-y, 1-z
C39-H39···N01	0.93	2.58	3.3350(12)	138	1+x, y, z
C58-H58···Cg7	0.93	2.92	3.718	144	-

	center...center	Symmetry code
$\pi(\text{Cg2})\cdots\pi(\text{Cg3})$	3.871	-x, -y, -z
$\pi(\text{Cg3})\cdots\pi(\text{Cg4})$	3.718	1-x,-y,-z
$\pi(\text{Cg2})\cdots\pi(\text{C11}\equiv\text{C12})$	3.284	1-x,-y,-z
$\pi(\text{Cg5})\cdots\pi(\text{Cg6})$	3.497	2-x,1-y,1-z
$\pi(\text{Cg6})\cdots\pi(\text{Cg7})$	3.879	1-x,1-y,1-z
$\pi(\text{Cg5})\cdots\pi(\text{C41}\equiv\text{C42})$	3.599	1-x,1-y,1-z

Cg2 is pyridine ring containing N1 atom, Cg3 is the pyridine ring containing N2 atom, Cg4 is the benzene ring containing C18 atom, Cg5 is pyridine ring containing N3 atom, Cg6 is pyridine ring containing N4 atom, Cg7 is the benzene ring containing C48 atom.

1 ·1/8(CH ₂ Cl ₂)		
	center...center	Symmetry code
$\pi(\text{Cg8})\cdots\pi(\text{C21}\equiv\text{C22})$	3.446	-x,1-y,1-z
$\pi(\text{Cg9})\cdots\pi(\text{C11}\equiv\text{C12})$	3.420	-x,1-y,1-z

Cg8 is the pyridine ring containing N1 atom, Cg9 is the pyridine ring containing N2 atom.

Table S4. Partial molecular orbital compositions (%) in the ground state for **1** in dichloromethane solution from the TD-DFT calculation.

orbital	energy (eV)	MO contribution (%)		
		Pt(s/p/d)	C≡CPh-Et-4	DiBrbpy
LUMO+11	0.60	52.2(0/52/48)	32.1	15.7
LUMO+8	-0.24	41.9(94/5/1)	56.3	1.8
LUMO+7	-0.02	2.6(17/20/63)	73.5	23.9
LUMO+6	-0.09	6.3(74/14/12)	5.4	88.3
LUMO+5	-0.14	4.7(2/34/64)	13.3	82.0
LUMO+4	-0.17	7.7(81/15/4)	12.7	79.6
LUMO+3	-0.26	18.2(5/73/22)	68.3	13.5
LUMO+2	-1.55	1.5(1/1/98)	0.7	97.8
LUMO+1	-1.79	2.8(0/59/41)	1.0	96.2
LUMO	-2.76	4.4(0/36/64)	2.6	93.0
HOMO	-5.67	16.1(0/1/99)	82.3	1.6
HOMO-1	-5.84	12.1(0/5/95)	85.0	2.9
HOMO-2	-6.34	33.9(0/1/99)	61.1	5.0
HOMO-3	-6.61	21.3(0/2/98)	73.4	5.3
HOMO-4	-6.87	96.4(28/0/72)	2.9	0.7
HOMO-5	-6.95	0.8(0/1/99)	99.1	0.1
HOMO-6	-7.02	0.05(4/4/92)	99.94	0.01
HOMO-7	-7.50	29.6(0/0/100)	59.4	11.0
HOMO-8	-7.81	12.3(0/2/98)	80.0	7.7
HOMO-9	-8.01	1.6(0/2/98)	10.2	88.2
HOMO-10	-8.13	9.8(0/1/99)	23.1	67.1

Table S5. Absorption and emission transition properties of **1** in dichloromethane solution by TD-DFT method at the PBE1PBE level with the polarized continuum model (PCM).

States	E , nm (eV)	O.S.	Component	Contri.	Assignment	Measured Wavelength (nm)
T_1	591 (2.10)	0.0000	HOMO→LUMO	91%	$^3\text{LLCT}/^3\text{MLCT}$	640
			HOMO-1→LUMO	7%	$^3\text{LLCT}/^3\text{MLCT}$	
S_2	517 (2.40)	0.0928	HOMO-1→LUMO	100%	$^1\text{LLCT}/^1\text{MLCT}$	469
S_3	453 (2.73)	0.1063	HOMO-2→LUMO	100%	$^1\text{LLCT}/^1\text{MLCT}$	429
S_5	405 (3.07)	0.0672	HOMO-3→LUMO	100%	$^1\text{LLCT}/^1\text{MLCT}$	291
S_8	356 (3.49)	0.1287	HOMO→LUMO+2	71%	$^1\text{LLCT}/^1\text{MLCT}$	279
			HOMO-1→LUMO+1	29%	$^1\text{LLCT}/^1\text{MLCT}$	
S_9	341 (3.63)	0.0721	HOMO-1→LUMO+2	100%	$^1\text{LLCT}/^1\text{MLCT}$	265
S_{19}	283 (4.38)	0.0695	HOMO-8→LUMO	96%	$^1\text{LLCT}/^1\text{MLCT}$	241
S_{20}	279 (4.45)	0.6633	HOMO-9→LUMO	53%	$^1\text{IL}/^1\text{LLCT}$	252
			HOMO-10→LUMO	35%	$^1\text{IL}/^1\text{LLCT}$	
			HOMO-3→LUMO+2	9%	$^1\text{LLCT}/^1\text{MLCT}$	
S_{21}	272 (4.55)	0.7132	HOMO→LUMO+3	100%	$^1\text{IL}/^1\text{MC}/^1\text{LLCT}$	291
S_{24}	262 (4.73)	0.2656	HOMO→LUMO+5	31%	$^1\text{IL}/^1\text{LLCT}/^1\text{MLCT}$	469
			HOMO→LUMO+11	21%	$^1\text{IL}/^1\text{MC}/^1\text{LLCT}$	
			HOMO-1→LUMO+3	19%	$^1\text{IL}/^1\text{MC}/^1\text{LLCT}$	
			HOMO→LUMO+4	11%	$^1\text{IL}/^1\text{LLCT}/^1\text{MLCT}$	
			HOMO→LUMO+6	11%	$^1\text{LLCT}/^1\text{MLCT}$	
S_{26}	260 (4.78)	0.0773	HOMO-1→LUMO+3	63%	$^1\text{IL}/^1\text{MC}/^1\text{LLCT}$	429
			HOMO-2→LUMO+3	12%	$^1\text{IL}/^1\text{MC}/^1\text{LLCT}$	
			HOMO→LUMO+5	11%	$^1\text{IL}/^1\text{LLCT}/^1\text{MLCT}$	
S_{30}	252 (4.92)	0.1779	HOMO-5→LUMO+2	26%	$^1\text{LLCT}$	241
			HOMO-1→LUMO+5	20%	$^1\text{IL}/^1\text{LLCT}/^1\text{MLCT}$	
			HOMO-1→LUMO+4	9%	$^1\text{IL}/^1\text{LLCT}/^1\text{MLCT}$	
			HOMO-1→LUMO+11	8%	$^1\text{IL}/^1\text{MC}/^1\text{LLCT}$	
			HOMO-1→LUMO+7	7%	$^1\text{IL}/^1\text{LLCT}/^1\text{MLCT}$	
S_{31}	252 (4.92)	0.1283	HOMO-2→LUMO+3	29%	$^1\text{IL}/^1\text{MC}/^1\text{LLCT}$	469
			HOMO-5→LUMO+2	13%	$^1\text{LLCT}$	
			HOMO-2→LUMO+7	11%	$^1\text{IL}/^1\text{LLCT}/^1\text{MLCT}$	
			HOMO→LUMO+6	11%	$^1\text{LLCT}/^1\text{MLCT}$	

S ₃₂	249 (4.99)	0.0819	HOMO-5→LUMO+2 HOMO→LUMO+8 HOMO-7→LUMO+1	36% 17% 13%	¹ LLCT ¹ IL/ ¹ MC/ ¹ LLCT ¹ IL/ ¹ LLCT/ ¹ MLCT
S ₃₆	246 (5.05)	0.1609	HOMO→LUMO+7 HOMO-3→LUMO+3 HOMO-1→LUMO+6 HOMO-6→LUMO+2 HOMO-1→LUMO+4 HOMO-1→LUMO+11 HOMO→LUMO+8	26% 12% 11% 10% 8% 8% 8%	¹ IL/ ¹ LLCT/ ¹ MLCT ¹ MC/ ¹ IL/ ¹ LLCT ¹ LLCT/ ¹ MLCT ¹ LLCT ¹ IL/ ¹ LLCT/ ¹ MLCT ¹ IL/ ¹ MC/ ¹ LLCT ¹ IL/ ¹ MC/ ¹ LLCT

Table S6. Partial molecular orbital compositions (%) in the ground state for the two-molecule model of **1**·DMSO in the solid state by TD-DFT method at the PBE1PBE level.

orbital	energy (eV)	MO contribution (%)		
		Pt(s/p/d)	C≡CPh-Et-4	DiBrbpy
LUMO+5	-1.29	2.85(21/52/27)	0.65	96.50
LUMO+4	-1.37	3.57(41/49/10)	1.18	95.25
LUMO+3	-1.63	2.85(4/59/37)	1.38	95.77
LUMO+2	-1.71	4.61(41/45/14)	2.54	92.85
LUMO+1	-2.54	3.89(7/28/65)	2.69	93.42
LUMO	-2.58	5.53(9/48/43)	2.83	91.64
HOMO	-5.35	14.10(2/2/96)	84.43	1.47
HOMO-1	-5.37	13.38(0/2/98)	85.13	1.49
HOMO-2	-5.58	15.04(0/5/95)	81.64	3.32
HOMO-3	-5.59	15.00(0/5/95)	80.96	4.04
HOMO-4	-5.95	32.96(1/1/98)	61.58	5.46
HOMO-5	-5.99	30.40(1/3/96)	64.28	5.32
HOMO-6	-6.29	22.97(6/3/91)	70.95	6.08
HOMO-7	-6.31	19.50(1/3/96)	76.69	3.81
HOMO-8	-6.54	86.65(28/0/72)	7.12	6.23
HOMO-9	-6.59	89.10(27/0/73)	3.62	7.28
HOMO-14	-7.31	27.67(0/1/99)	61.52	10.81
HOMO-15	-7.34	27.50(1/0/99)	60.82	11.68

Table S7. Absorption and emission transition properties for the two-molecule model of **1**·DMSO in the solid state by TD-DFT method at the PBE1PBE level.

States	E , nm (eV)	O.S.	Component	Contri.	Assignment	Measured Wavelength (nm)
T_1	617 (2.01)	0.0000	HOMO→LUMO	72%	$^3\text{LLCT}/^3\text{MLCT}$	570
			HOMO-1→LUMO+1	20%	$^3\text{LLCT}/^3\text{MLCT}$	
T_2	613 (2.02)	0.0000	HOMO-1→LUMO	48%	$^3\text{LLCT}/^3\text{MLCT}$	
			HOMO→LUMO+1	45%	$^3\text{LLCT}/^3\text{MLCT}$	
T_3	581 (2.14)	0.0000	HOMO-1→LUMO	35%	$^3\text{LLCT}/^3\text{MLCT}$	
			HOMO→LUMO+1	31%	$^3\text{LLCT}/^3\text{MLCT}$	
			HOMO-2→LUMO+1	18%	$^3\text{LLCT}/^3\text{MLCT}$	
			HOMO-3→LUMO	15%	$^3\text{LLCT}/^3\text{MLCT}$	
S_6	529 (2.34)	0.0446	HOMO-3→LUMO	84%	$^1\text{LLCT}/^1\text{MLCT}$	501
			HOMO-2→LUMO	8%	$^1\text{LLCT}/^1\text{MLCT}$	
			HOMO→LUMO+1	8%	$^1\text{LLCT}/^1\text{MLCT}$	
S_8	524 (2.37)	0.0412	HOMO-2→LUMO+1	81%	$^1\text{LLCT}/^1\text{MLCT}$	
			HOMO→LUMO+1	9%	$^1\text{LLCT}/^1\text{MLCT}$	
S_{10}	475 (2.61)	0.1298	HOMO-4→LUMO	71%	$^1\text{LLCT}/^1\text{MLCT}$	462
			HOMO-5→LUMO+1	21%	$^1\text{LLCT}/^1\text{MLCT}$	
S_{16}	418 (2.96)	0.0380	HOMO-7→LUMO	70%	$^1\text{LLCT}/^1\text{MLCT}$	412
			HOMO-6→LUMO+1	12%	$^1\text{LLCT}/^1\text{MLCT}$	
			HOMO-1→LUMO+2	12%	$^1\text{LLCT}/^1\text{MLCT}$	
S_{24}	383 (3.24)	0.0338	HOMO-3→LUMO+2	61%	$^1\text{LLCT}/^1\text{MLCT}$	385
			HOMO→LUMO+3	16%	$^1\text{LLCT}/^1\text{MLCT}$	
			HOMO-1→LUMO+2	7%	$^1\text{LLCT}/^1\text{MLCT}$	
S_{27}	377 (3.29)	0.0582	HOMO-9→LUMO	36%	$^1\text{MLCT}$	
			HOMO-8→LUMO+1	33%	$^1\text{MLCT}$	
			HOMO-2→LUMO+3	14%	$^1\text{LLCT}/^1\text{MLCT}$	
			HOMO-1→LUMO+4	11%	$^1\text{LLCT}/^1\text{MLCT}$	
S_{31}	363 (3.41)	0.0500	HOMO→LUMO+5	41%	$^1\text{LLCT}/^1\text{MLCT}$	
			HOMO-1→LUMO+4	24%	$^1\text{LLCT}/^1\text{MLCT}$	
			HOMO-4→LUMO+2	18%	$^1\text{LLCT}/^1\text{MLCT}$	
			HOMO-2→LUMO+3	9%	$^1\text{LLCT}/^1\text{MLCT}$	
S_{33}	358 (3.46)	0.0477	HOMO-4→LUMO+2	56%	$^1\text{LLCT}/^1\text{MLCT}$	
			HOMO-5→LUMO+3	18%	$^1\text{LLCT}/^1\text{MLCT}$	
			HOMO-2→LUMO+3	10%	$^1\text{LLCT}/^1\text{MLCT}$	

			HOMO→LUMO+5	8%	$^1\text{LLCT}/^1\text{MLCT}$	
			HOMO-1→LUMO+4	8%	$^1\text{LLCT}/^1\text{MLCT}$	
S ₃₈	344 (3.60)	0.0422	HOMO-2→LUMO+5	83%	$^1\text{LLCT}/^1\text{MLCT}$	344
			HOMO-3→LUMO+4	9%	$^1\text{LLCT}/^1\text{MLCT}$	
			HOMO→LUMO+5	8%	$^1\text{LLCT}/^1\text{MLCT}$	
S ₄₉	321 (3.87)	0.0348	HOMO-4→LUMO+4	36%	$^1\text{LLCT}/^1\text{MLCT}$	315
			HOMO-7→LUMO+2	36%	$^1\text{LLCT}/^1\text{MLCT}$	
			HOMO-6→LUMO+3	10%	$^1\text{LLCT}/^1\text{MLCT}$	
S ₅₆	313 (3.96)	0.0392	HOMO-5→LUMO+5	76%	$^1\text{LLCT}/^1\text{MLCT}$	
S ₅₉	307 (4.04)	0.0349	HOMO-14→LUMO	71%	$^1\text{IL}/^1\text{LLCT}/^1\text{MLCT}$	300
			HOMO-15→LUMO+1	9%	$^1\text{IL}/^1\text{LLCT}/^1\text{MLCT}$	

Table S8. Partial molecular orbital compositions (%) in the ground state for the two-molecule model of **1**·**1/2(CH₃CN)** in the solid state by TD-DFT method at the PBE1PBE level.

orbital	energy (eV)	MO contribution (%)		
		Pt(s/p/d)	C≡CPh-Et-4	DiBrbpy
LUMO+5	-1.41	2.86(48/24/28)	1.89	95.25
LUMO+4	-1.44	3.16(29/56/15)	2.72	94.12
LUMO+3	-1.70	2.17(5/50/45)	0.44	97.39
LUMO+2	-1.73	2.71(27/52/21)	2.81	94.48
LUMO+1	-2.51	4.78(5/22/73)	4.67	90.55
LUMO	-2.59	5.60(6/41/53)	4.31	90.09
HOMO	-5.26	17.01(1/1/98)	79.72	3.27
HOMO-1	-5.29	16.92(1/1/98)	80.88	2.20
HOMO-2	-5.46	18.06(1/8/91)	75.79	6.15
HOMO-3	-5.48	17.91(0/9/91)	74.67	7.42
HOMO-12	-6.94	10.39(10/8/82)	82.02	7.59
HOMO-13	-6.97	6.17(5/4/91)	87.88	5.95
HOMO-14	-7.03	34.77(0/0/100)	49.72	15.51
HOMO-15	-7.04	37.77(0/0/100)	45.76	16.47
HOMO-16	-7.16	23.54(3/1/96)	64.55	11.91

Table S9. Absorption and emission transition properties for the two-molecule model of **1**·1/2(CH₃CN) in the solid state by TD-DFT method at the PBE1PBE level.

States	<i>E</i> , nm (eV)	O.S.	Component	Contri.	Assignment	Measured Wavelength (nm)
T ₁	683 (1.82)	0.0000	HOMO→LUMO	78%	³ LLCT/ ³ MLCT	625
			HOMO-1→LUMO+1	15%	³ LLCT/ ³ MLCT	
T ₂	674 (1.84)	0.0000	HOMO-1→LUMO	50%	³ LLCT/ ³ MLCT	
			HOMO→LUMO+1	40%	³ LLCT/ ³ MLCT	
			HOMO-3→LUMO	7%	³ LLCT/ ³ MLCT	
T ₃	624 (1.99)	0.0000	HOMO→LUMO+1	45%	³ LLCT/ ³ MLCT	
			HOMO-1→LUMO	43%	³ LLCT/ ³ MLCT	
			HOMO-2→LUMO+1	12%	³ LLCT/ ³ MLCT	
S ₂	618 (2.00)	0.0365	HOMO-1→LUMO	85%	¹ LLCT/ ¹ MLCT	582
S ₃	602 (2.06)	0.0591	HOMO→LUMO+1	88%	¹ LLCT/ ¹ MLCT	
			HOMO-1→LUMO	8%	¹ LLCT/ ¹ MLCT	
S ₆	532 (2.33)	0.1883	HOMO-3→LUMO	92%	¹ LLCT/ ¹ MLCT	530
			HOMO→LUMO+1	96%	¹ LLCT/ ¹ MLCT	
S ₈	521 (2.38)	0.1427	HOMO-2→LUMO+1	96%	¹ LLCT/ ¹ MLCT	
S ₁₇	424 (2.93)	0.0576	HOMO→LUMO+3	79%	¹ LLCT/ ¹ MLCT	430
			HOMO-1→LUMO+2	17%	¹ LLCT/ ¹ MLCT	
S ₂₆	388 (3.19)	0.1123	HOMO-1→LUMO+4	48%	¹ LLCT/ ¹ MLCT	390
			HOMO-3→LUMO+2	27%	¹ LLCT/ ¹ MLCT	
			HOMO→LUMO+5	15%	¹ LLCT/ ¹ MLCT	
			HOMO-2→LUMO+5	7%	¹ LLCT/ ¹ MLCT	
			HOMO-2→LUMO+3	47%	¹ LLCT/ ¹ MLCT	
S ₂₈	384 (3.23)	0.0346	HOMO-3→LUMO+4	20%	¹ LLCT/ ¹ MLCT	
			HOMO-3→LUMO+2	13%	¹ LLCT/ ¹ MLCT	
			HOMO-1→LUMO+4	8%	¹ LLCT/ ¹ MLCT	
			HOMO-1→LUMO+2	7%	¹ LLCT/ ¹ MLCT	
			HOMO-3→LUMO+4	45%	¹ LLCT/ ¹ MLCT	346
S ₃₆	361 (3.43)	0.1556	HOMO-2→LUMO+5	36%	¹ LLCT/ ¹ MLCT	
			HOMO-1→LUMO+4	9%	¹ LLCT/ ¹ MLCT	
			HOMO-1→LUMO+2	7%	¹ LLCT/ ¹ MLCT	
S ₄₂	346 (3.59)	0.0396	HOMO-13→LUMO	58%	¹ LLCT	
			HOMO-12→LUMO+1	42%	¹ LLCT/ ¹ MLCT	
S ₅₃	322 (3.85)	0.0675	HOMO-16→LUMO	54%	¹ IL/ ¹ LLCT/ ¹ MLCT	323
			HOMO-13→LUMO	15%	¹ LLCT	
			HOMO-12→LUMO+1	9%	¹ LLCT/ ¹ MLCT	
			HOMO-15→LUMO	9%	¹ IL/ ¹ LLCT/ ¹ MLCT	
			HOMO-14→LUMO+1	7%	¹ IL/ ¹ LLCT/ ¹ MLCT	

Table S10. Partial molecular orbital compositions (%) in the ground state for the two-molecule model of **1·1/8(CH₂Cl₂)** in the solid state by TD-DFT method at the PBE1PBE level.

orbital	energy (eV)	MO contribution (%)		
		Pt(s/p/d)	C≡CC ₆ H ₄ Et-4	DiBrbpy
LUMO+5	-1.29	2.35(3/81/16)	0.06	97.59
LUMO+4	-1.30	2.57(50/12/38)	2.48	94.95
LUMO+3	-1.43	3.19(81/9/10)	1.20	95.61
LUMO+2	-1.63	4.51(25/57/18)	1.11	94.38
LUMO+1	-2.41	3.71(39/15/46)	2.88	93.41
LUMO	-2.51	6.91(9/41/50)	4.30	88.79
HOMO	-5.25	19.85(0/6/94)	77.89	2.26
HOMO-1	-5.37	43.53(21/1/78)	53.48	2.99
HOMO-2	-5.39	16.44(2/1/97)	81.46	2.10
HOMO-3	-5.48	21.29(2/8/90)	71.81	6.90
HOMO-4	-5.86	63.36(23/3/74)	31.95	4.69
HOMO-9	-6.69	1.78(0/10/90)	96.67	1.55
HOMO-10	-6.70	1.85(4/5/91)	96.30	1.85
HOMO-11	-6.71	5.47(1/1/98)	90.17	4.36
HOMO-12	-6.74	3.49(6/6/88)	95.73	0.78
HOMO-13	-7.06	33.09(0/0/100)	45.71	21.20
HOMO-14	-7.10	30.04(2/1/97)	50.88	19.08
HOMO-15	-7.13	53.62(13/0/87)	41.60	4.78
HOMO-16	-7.15	48.90(13/1/86)	48.14	2.96
HOMO-17	-7.26	64.47(20/0/80)	23.60	11.93

Table S11. Absorption and emission transition properties for the two-molecule model of **1·1/8(CH₂Cl₂)** in the solid state by TD-DFT method at the PBE1PBE level.

States	E, nm (eV)	O.S.	Component	Contri.	Assignment	Measured Wavelength (nm)
T ₁	655 (1.89)	0.0000	HOMO→LUMO	100%	³ MMLCT/ ³ LLCT	1022
S ₁	623 (1.99)	0.0000	HOMO→LUMO	100%	¹ MLCT/ ¹ LLCT	761
S ₂	612 (2.02)	0.0250	HOMO-1→LUMO	87%	¹ MLCT/ ¹ LLCT	
			HOMO-4→LUMO	8%	¹ MLCT/ ¹ LLCT	
S ₅	573 (2.17)	0.0637	HOMO-2→LUMO	88%	¹ MLCT/ ¹ LLCT	670
			HOMO→LUMO+1	9%	¹ MLCT/ ¹ LLCT	
S ₈	521 (2.38)	0.0985	HOMO-3→LUMO+1	91%	¹ MLCT/ ¹ LLCT	534
			HOMO-4→LUMO	9%	¹ MLCT/ ¹ LLCT	
S ₉	487 (2.55)	0.1741	HOMO-4→LUMO	84%	¹ MLCT/ ¹ LLCT	494
			HOMO-1→LUMO	11%	¹ MLCT/ ¹ LLCT	
S ₁₉	398 (3.12)	0.0239	HOMO→LUMO+3	73%	¹ MLCT/ ¹ LLCT	423
			HOMO-2→LUMO+2	22%	¹ MLCT/ ¹ LLCT	
S ₂₄	384 (3.23)	0.0508	HOMO→LUMO+4	62%	¹ MLCT/ ¹ LLCT	
			HOMO-1→LUMO+5	21%	¹ MLCT/ ¹ LLCT	
S ₃₀	374 (3.32)	0.0323	HOMO-1→LUMO+5	41%	¹ MLCT/ ¹ LLCT	
			HOMO-3→LUMO+3	27%	¹ MLCT/ ¹ LLCT	
			HOMO→LUMO+4	24%	¹ MLCT/ ¹ LLCT	
S ₃₂	361 (3.43)	0.0586	HOMO-3→LUMO+4	36%	¹ MLCT/ ¹ LLCT	356
			HOMO-2→LUMO+5	28%	¹ MLCT/ ¹ LLCT	
			HOMO-3→LUMO+3	18%	¹ MLCT/ ¹ LLCT	
			HOMO-4→LUMO+2	16%	¹ MLCT/ ¹ LLCT	
S ₃₃	358.09 (3.46)	0.0995	HOMO-4→LUMO+2	76%	¹ MLCT/ ¹ LLCT	
			HOMO-2→LUMO+5	7%	¹ MLCT/ ¹ LLCT	
			HOMO→LUMO+4	7%	¹ MLCT/ ¹ LLCT	
S ₃₅	354 (3.50)	0.0858	HOMO-3→LUMO+4	55%	¹ MLCT/ ¹ LLCT	
			HOMO-2→LUMO+5	33%	¹ MLCT/ ¹ LLCT	
			HOMO-3→LUMO+3	7%	¹ MLCT/ ¹ LLCT	
S ₃₉	344 (3.61)	0.0358	HOMO-11→LUMO	74%	¹ LLCT	
			HOMO-10→LUMO	11%	¹ LLCT	
			HOMO-13→LUMO	8%	¹ IL/ ¹ LLCT/ ¹ MLCT	
S ₄₈	328 (3.78)	0.0209	HOMO-4→LUMO+5	80%	¹ MLCT/ ¹ LLCT	310
			HOMO-9→LUMO+1	13%	¹ LLCT	
S ₅₂	325 (3.82)	0.0203	HOMO-17→LUMO+1	30%	¹ IL/ ¹ LLCT/ ¹ MLCT	
			HOMO-15→LUMO+1	25%	¹ MLCT/ ¹ LLCT	
			HOMO-16→LUMO+1	22%	¹ MLCT/ ¹ LLCT	

			HOMO-13→LUMO	10%	$^1\text{IL}/^1\text{LLCT}/^1\text{MLCT}$
S ₅₃	321 (3.86)	0.0228	HOMO-13→LUMO	44%	$^1\text{IL}/^1\text{LLCT}/^1\text{MLCT}$
			HOMO-12→LUMO+1	29%	$^1\text{LLCT}$
			HOMO-11→LUMO	13%	$^1\text{LLCT}$
			HOMO-14→LUMO	12%	$^1\text{IL}/^1\text{LLCT}/^1\text{MLCT}$
S ₆₀	313 (3.96)	0.0465	HOMO-14→LUMO	86%	$^1\text{IL}/^1\text{LLCT}/^1\text{MLCT}$

Table S12. Partial molecular orbital compositions (%) in the ground state for the three-molecule model of **1·1/8(CH₂Cl₂)** in the solid state by TD-DFT method at the PBE1PBE level.

orbital	energy (eV)	MO contribution (%)		
		Pt(s/p/d)	C≡CPh-Et-4	DiBrbpy
LUMO+7	-1.15	4.36(24/50/26)	1.99	93.65
LUMO+6	-1.29	2.78(16/79/5)	1.43	95.79
LUMO+5	-1.32	2.45(9/77/14)	1.83	95.72
LUMO+4	-1.53	4.38(55/38/7)	1.29	94.33
LUMO+3	-1.59	4.28(7/91/2)	43.87	51.85
LUMO+2	-2.07	4.31(19/37/44)	4.25	91.44
LUMO+1	-2.45	5.22(75/18/7)	4.54	90.24
LUMO	-2.54	6.70(42/49/9)	4.53	88.77
HOMO	-5.16	54.74(31/0/69)	42.55	2.71
HOMO-1	-5.18	19.09(3/9/88)	78.59	2.32
HOMO-2	-5.23	24.54(21/8/71)	72.97	2.49
HOMO-3	-5.40	22.50(6/5/89)	70.76	6.74
HOMO-4	-5.45	18.65(1/2/97)	77.73	3.62
HOMO-5	-5.59	42.24(24/3/73)	50.86	6.90
HOMO-6	-5.61	33.81(4/3/93)	60.90	5.29

Table S13. Absorption and emission transition properties for the three-molecule model of **1·1/8(CH₂Cl₂)** in the solid state by TD-DFT method at the PBE1PBE level.

States	<i>E</i> , nm (eV)	O.S.	Component	Contri.	Assignment	Measured Wavelength (nm)
T ₁	707 (1.75)	0.0000	HOMO→LUMO	94%	³ MMLCT/ ³ LLCT	1022
S ₁	666 (1.86)	0.0271	HOMO→LUMO	84%	¹ MLCT/ ¹ LLCT	761
			HOMO-2→LUMO	9%	¹ MLCT/ ¹ LLCT	
S ₂	641 (1.93)	0.0152	HOMO→LUMO+1	79%	¹ MLCT/ ¹ LLCT	670
			HOMO-2→LUMO+1	8%	¹ MLCT/ ¹ LLCT	
			HOMO-5→LUMO+1	7%	¹ MLCT/ ¹ LLCT	
S ₃	631 (1.96)	0.0263	HOMO-2→LUMO	50%	¹ MLCT/ ¹ LLCT	
			HOMO-1→LUMO	37%	¹ MLCT/ ¹ LLCT	
			HOMO→LUMO	7%	¹ MLCT/ ¹ LLCT	
S ₆	563 (2.20)	0.0321	HOMO-3→LUMO	36%	¹ MLCT/ ¹ LLCT	534
			HOMO-4→LUMO+1	18%	¹ MLCT/ ¹ LLCT	
			HOMO-4→LUMO	13%	¹ MLCT/ ¹ LLCT	
			HOMO-3→LUMO+1	10%	¹ MLCT/ ¹ LLCT	
			HOMO-2→LUMO+1	8%	¹ MLCT/ ¹ LLCT	
			HOMO-6→LUMO	8%	¹ MLCT/ ¹ LLCT	
S ₁₀	536 (2.31)	0.0331	HOMO-3→LUMO+1	45%	¹ MLCT/ ¹ LLCT	
			HOMO-2→LUMO+1	22%	¹ MLCT/ ¹ LLCT	
			HOMO-5→LUMO	13%	¹ MLCT/ ¹ LLCT	
			HOMO-5→LUMO+1	10%	¹ MLCT/ ¹ LLCT	
S ₁₂	525 (2.36)	0.0578	HOMO-6→LUMO	49%	¹ MLCT/ ¹ LLCT	
			HOMO-5→LUMO	16%	¹ MLCT/ ¹ LLCT	
			HOMO-3→LUMO	14%	¹ MLCT/ ¹ LLCT	
			HOMO-4→LUMO	10%	¹ MLCT/ ¹ LLCT	
S ₁₆	499 (2.48)	0.0736	HOMO-6→LUMO+1	54%	¹ MLCT/ ¹ LLCT	494
			HOMO-5→LUMO	14%	¹ MLCT/ ¹ LLCT	
			HOMO-3→LUMO+1	11%	¹ MLCT/ ¹ LLCT	
			HOMO-5→LUMO+1	8%	¹ MLCT/ ¹ LLCT	
			HOMO-2→LUMO+2	8%	¹ MLCT/ ¹ LLCT	
S ₁₉	479 (2.60)	0.0249	HOMO-5→LUMO+1	53%	¹ MLCT/ ¹ LLCT	
			HOMO-3→LUMO+1	19%	¹ MLCT/ ¹ LLCT	
			HOMO-4→LUMO+1	11%	¹ MLCT/ ¹ LLCT	
			HOMO-3→LUMO+2	9%	¹ MLCT/ ¹ LLCT	
S ₂₀	467 (2.66)	0.0305	HOMO-3→LUMO+2	78%	¹ MLCT/ ¹ LLCT	
			HOMO-4→LUMO+2	15%	¹ MLCT/ ¹ LLCT	
S ₂₄	440 (2.82)	0.0626	HOMO-6→LUMO+2	88%	¹ MLCT/ ¹ LLCT	423
			HOMO-5→LUMO+2	9%	¹ MLCT/ ¹ LLCT	

					¹ MLCT/ ¹ LLCT	
S ₄₅	385 (3.22)	0.0205	HOMO-1→LUMO+6	21%	¹ MLCT/ ¹ LLCT	
			HOMO-4→LUMO+3	18%	¹ MLCT/ ¹ LLCT	
			HOMO-5→LUMO+3	13%	¹ IL/ ¹ MLCT/ ¹ LLCT	
			HOMO-3→LUMO+4	10%	¹ MLCT/ ¹ LLCT	
			HOMO-6→LUMO+3	9%	¹ IL/ ¹ MLCT/ ¹ LLCT	
			HOMO-1→LUMO+7	8%	¹ MLCT/ ¹ LLCT	
S ₄₇	384 (3.23)	0.0233	HOMO-2→LUMO+5	26%	¹ MLCT/ ¹ LLCT	
			HOMO-1→LUMO+5	26%	¹ MLCT/ ¹ LLCT	
			HOMO-3→LUMO+4	13%	¹ MLCT/ ¹ LLCT	
			HOMO-6→LUMO+3	13%	¹ IL/ ¹ LLCT/ ¹ MLCT	
S ₅₂	375 (3.31)	0.0549	HOMO-6→LUMO+3	47%	¹ IL/ ¹ LLCT/ ¹ MLCT	356
			HOMO-5→LUMO+3	16%	¹ IL/ ¹ LLCT/ ¹ MLCT	
			HOMO-2→LUMO+5	8%	¹ MLCT/ ¹ LLCT	
			HOMO-4→LUMO+3	8%	¹ IL/ ¹ LLCT/ ¹ MLCT	

Table S14. Partial molecular orbital compositions (%) in the ground state for the four-molecule model of **1·1/8(CH₂Cl₂)** in the solid state by TD-DFT method at the PBE1PBE level.

orbital	energy (eV)	MO contribution (%)		
		Pt(s/p/d)	C≡CPh-Et-4	DiBrbpy
LUMO+7	-1.24	26.97(9/85/6)	2.76	70.27
LUMO+6	-1.25	17.91(8/81/11)	3.21	78.88
LUMO+5	-1.48	54.02(46/51/3)	2.15	43.83
LUMO+4	-1.51	40.47(38/52/10)	4.84	54.69
LUMO+3	-1.93	21.09(83/5/12)	4.97	73.94
LUMO+2	-2.20	12.58(43/32/25)	5.23	82.19
LUMO+1	-2.39	19.96(58/21/21)	3.93	76.11
LUMO	-2.41	13.70(22/46/32)	3.96	82.34
HOMO	-4.98	84.63(30/3/67)	12.08	3.29
HOMO-1	-5.14	30.28(5/5/90)	66.10	3.62
HOMO-2	-5.16	28.15(1/7/92)	68.52	3.33
HOMO-3	-5.31	43.84(16/5/79)	51.33	4.83
HOMO-4	-5.32	28.18(4/4/92)	67.48	4.34
HOMO-5	-5.36	36.33(8/5/87)	55.70	7.97
HOMO-6	-5.41	27.94(1/3/96)	67.05	5.01
HOMO-7	-5.46	46.86(24/7/69)	45.29	7.85
HOMO-8	-5.54	34.15(11/9/80)	58.41	7.44
HOMO-9	-5.88	43.56(6/4/90)	52.02	4.42
HOMO-10	-5.89	39.93(0/3/97)	55.46	4.61

Table S15. Absorption and emission transition properties for the four-molecule model of **1·1/8(CH₂Cl₂)** in the solid state by TD-DFT method at the PBE1PBE level.

States	<i>E</i> , nm (eV)	O.S.	Component	Contri.	Assignment	Measured Wavelength (nm)
T ₁	719 (1.73)	0.0000	HOMO→LUMO	77%	³ MMLCT/ ³ LLCT/ ³ MC	1022
			HOMO→LUMO+2	10%	³ MMLCT/ ³ LLCT/ ³ MC	
			HOMO-3→LUMO+1	7%	³ MMLCT/ ³ LLCT/ ³ MC	
S ₁	681 (1.82)	0.0608	HOMO→LUMO	81%	¹ MLCT/ ¹ LLCT/ ¹ MC	761
			HOMO→LUMO+2	7%	¹ MLCT/ ¹ LLCT/ ¹ MC	
S ₅	612 (2.03)	0.0289	HOMO-2→LUMO	48%	¹ MLCT/ ¹ LLCT/ ¹ MC	670
			HOMO-1→LUMO+1	48%	¹ MLCT/ ¹ LLCT/ ¹ MC	
S ₁₄	521 (2.38)	0.0967	HOMO-3→LUMO+1	45%	¹ MLCT/ ¹ LLCT/ ¹ MC	534
			HOMO-7→LUMO	22%	¹ MLCT/ ¹ LLCT/ ¹ MC	
			HOMO-4→LUMO+2	14%	¹ MLCT/ ¹ LLCT/ ¹ MC	
S ₁₅	518 (2.39)	0.0413	HOMO-4→LUMO+2	55%	¹ MLCT/ ¹ LLCT/ ¹ MC	
			HOMO-3→LUMO+1	11%	¹ MLCT/ ¹ LLCT/ ¹ MC	
			HOMO-2→LUMO+3	8%	¹ MLCT/ ¹ LLCT/ ¹ MC	
S ₁₉	505 (2.46)	0.0203	HOMO-6→LUMO+2	34%	¹ MLCT/ ¹ LLCT/ ¹ MC	
			HOMO-5→LUMO+2	15%	¹ MLCT/ ¹ LLCT/ ¹ MC	
			HOMO-4→LUMO+1	11%	¹ MLCT/ ¹ LLCT/ ¹ MC	
			HOMO-2→LUMO	11%	¹ MLCT/ ¹ LLCT/ ¹ MC	
			HOMO-1→LUMO+1	11%	¹ MLCT/ ¹ LLCT/ ¹ MC	
S ₂₁	488 (2.5)	0.0348	HOMO-5→LUMO+1	29%	¹ MLCT/ ¹ LLCT/ ¹ MC	494
			HOMO-2→LUMO+2	16%	¹ MLCT/ ¹ LLCT/ ¹ MC	
			HOMO-4→LUMO	15%	¹ MLCT/ ¹ LLCT/ ¹ MC	
			HOMO-8→LUMO	13%	¹ MLCT/ ¹ LLCT/ ¹ MC	
			HOMO-8→LUMO+2	7%	¹ MLCT/ ¹ LLCT/ ¹ MC	
S ₂₄	482 (2.57)	0.0342	HOMO-6→LUMO+1	20%	¹ MLCT/ ¹ LLCT/ ¹ MC	
			HOMO-8→LUMO	17%	¹ MLCT/ ¹ LLCT/ ¹ MC	
			HOMO-9→LUMO+1	11%	¹ MLCT/ ¹ LLCT/ ¹ MC	
			HOMO-10→LUMO	11%	¹ MLCT/ ¹ LLCT/ ¹ MC	
			HOMO-8→LUMO+2	10%	¹ MLCT/ ¹ LLCT/ ¹ MC	
			HOMO-4→LUMO+2	10%	¹ MLCT/ ¹ LLCT/ ¹ MC	
			HOMO-4→LUMO	8%	¹ MLCT/ ¹ LLCT/ ¹ MC	
S ₃₂	460 (2.67)	0.0291	HOMO-8→LUMO+2	45%	¹ MLCT/ ¹ LLCT/ ¹ MC	
			HOMO-8→LUMO	17%	¹ MLCT/ ¹ LLCT/ ¹ MC	
			HOMO-6→LUMO+1	10%	¹ MLCT/ ¹ LLCT/ ¹ MC	
			HOMO-7→LUMO	8%	¹ MLCT/ ¹ LLCT/ ¹ MC	
			HOMO-7→LUMO+2	7%	¹ MLCT/ ¹ LLCT/ ¹ MC	
S ₃₃	457	0.0854	HOMO-3→LUMO+3	45%	¹ MLCT/ ¹ LLCT/ ¹ MC	
			HOMO-5→LUMO+3	37%	¹ MLCT/ ¹ LLCT/ ¹ MC	

	(2.69)		HOMO-6→LUMO+3	7%	¹ MLCT/ ¹ LLCT/ ¹ MC	
S ₃₆	447 (2.77)	0.0304	HOMO→LUMO+4	83%	¹ MLCT/ ¹ LLCT/ ¹ MC	
S ₄₁	431 (2.88)	0.0185	HOMO-5→LUMO+3	33%	¹ MLCT/ ¹ LLCT/ ¹ MC	423
			HOMO-3→LUMO+3	31%	¹ MLCT/ ¹ LLCT/ ¹ MC	
			HOMO-7→LUMO+2	15%	¹ MLCT/ ¹ LLCT/ ¹ MC	

Table S16. Partial molecular orbital compositions (%) in the ground state for the five-molecule model of **1·1/8(CH₂Cl₂)** in the solid state by TD-DFT method at the PBE1PBE level.

orbital	energy (eV)	MO contribution (%)		
		Pt(s/p/d)	C≡CPh-Et-4	DiBrbpy
LUMO+6	-1.48	46.45(45/49/6)	3.34	50.21
LUMO+5	-1.50	44.65(27/67/6)	3.14	52.30
LUMO+4	-1.90	21.45(75/12/13)	4.80	73.75
LUMO+3	-2.00	22.51(65/22/13)	4.93	72.56
LUMO+2	-2.19	27.90(60/29/11)	4.40	67.70
LUMO+1	-2.39	19.15(51/27/22)	3.97	76.88
LUMO	-2.46	24.84(69/17/14)	4.44	70.72
HOMO	-4.89	88.39(31/1/68)	8.19	3.42
HOMO-1	-5.12	30.02(4/5/91)	66.32	3.66
HOMO-2	-5.14	31.84(11/6/83)	64.22	3.94
HOMO-3	-5.21	32.21(6/7/87)	63.23	4.56
HOMO-4	-5.22	58.98(20/6/74)	38.09	2.93
HOMO-5	-5.33	30.59(5/9/86)	61.55	7.86
HOMO-6	-5.35	29.17(6/6/88)	65.31	5.52
HOMO-7	-5.37	26.24(6/4/90)	68.04	5.72
HOMO-8	-5.42	38.85(18/8/74)	53.00	8.15
HOMO-9	-5.46	40.55(11/7/82)	53.48	5.97
HOMO-10	-5.52	36.09(15/7/78)	56.50	7.41
HOMO-11	-5.77	70.82(24/4/72)	21.78	7.40

Table S17. Absorption and emission transition properties for the five-molecule model of **1·1/8(CH₂Cl₂)** in the solid state by TD-DFT method at the PBE1PBE level.

States	<i>E</i> , nm (eV)	O.S.	Component	Contri.	Assignment	Measured Wavelength (nm)
T ₁	742 (1.67)	0.0000	HOMO→LUMO	65%	³ MMLCT/ ³ LLCT/ ³ MC	1022
			HOMO→LUMO+2	11%		
S ₁	708 (1.75)	0.0715	HOMO→LUMO	73%	¹ MLCT/ ¹ LLCT/ ¹ MC	761
			HOMO→LUMO+2	8%	¹ MLCT/ ¹ LLCT/ ¹ MC	
S ₂	684 (1.81)	0.0171	HOMO→LUMO+1	70%	¹ MLCT/ ¹ LLCT/ ¹ MC	670
			HOMO-4→LUMO+1	7%	¹ MLCT/ ¹ LLCT/ ¹ MC	
S ₁₄	542 (2.29)	0.049	HOMO-8→LUMO	24%	¹ MLCT/ ¹ LLCT/ ¹ MC	534
			HOMO-4→LUMO	17%	¹ MLCT/ ¹ LLCT/ ¹ MC	
			HOMO-2→LUMO+2	9%	¹ MLCT/ ¹ LLCT/ ¹ MC	
			HOMO-3→LUMO+2	8%	¹ MLCT/ ¹ LLCT/ ¹ MC	
S ₆	529 (2.34)	0.074	HOMO-5→LUMO+1	24%	¹ MLCT/ ¹ LLCT/ ¹ MC	
			HOMO-4→LUMO+1	21%	¹ MLCT/ ¹ LLCT/ ¹ MC	
			HOMO-8→LUMO+1	14%	¹ MLCT/ ¹ LLCT/ ¹ MC	
			HOMO-6→LUMO+1	14%	¹ MLCT/ ¹ LLCT/ ¹ MC	
S ₂₆	493 (2.52)	0.0431	HOMO-5→LUMO+2	17%	¹ MLCT/ ¹ LLCT/ ¹ MC	494
			HOMO-3→LUMO+3	12%	¹ MLCT/ ¹ LLCT/ ¹ MC	
			HOMO-9→LUMO+1	7%	¹ MLCT/ ¹ LLCT/ ¹ MC	
			HOMO-6→LUMO+2	6%	¹ MLCT/ ¹ LLCT/ ¹ MC	
			HOMO-10→LUMO+1	5%	¹ MLCT/ ¹ LLCT/ ¹ MC	
S ₄₀	466 (2.66)	0.0343	HOMO-4→LUMO+4	37%	¹ MLCT/ ¹ LLCT/ ¹ MC	
			HOMO-7→LUMO+3	13%	¹ MLCT/ ¹ LLCT/ ¹ MC	
			HOMO-10→LUMO+2	6%	¹ MLCT/ ¹ LLCT/ ¹ MC	
S ₄₅	452 (2.74)	0.0376	HOMO→LUMO+5	49%	¹ MLCT/ ¹ LLCT/ ¹ MC	
			HOMO→LUMO+6	24%	¹ MLCT/ ¹ LLCT/ ¹ MC	
S ₄₆	450 (2.76)	0.0258	HOMO-11→LUMO	23%	¹ MLCT/ ¹ LLCT/ ¹ MC	
			HOMO→LUMO+6	10%	¹ MLCT/ ¹ LLCT/ ¹ MC	
			HOMO-10→LUMO+1	8%	¹ MLCT/ ¹ LLCT/ ¹ MC	
			HOMO-8→LUMO+3	8%	¹ MLCT/ ¹ LLCT/ ¹ MC	
			HOMO-11→LUMO+2	7%	¹ MLCT/ ¹ LLCT/ ¹ MC	
S ₄₈	449 (2.76)	0.0291	HOMO-11→LUMO	12%	¹ MLCT/ ¹ LLCT/ ¹ MC	
			HOMO-6→LUMO+4	11%	¹ MLCT/ ¹ LLCT/ ¹ MC	
			HOMO→LUMO+6	11%	¹ MLCT/ ¹ LLCT/ ¹ MC	
			HOMO-8→LUMO+2	8%	¹ MLCT/ ¹ LLCT/ ¹ MC	
S ₅₁	444 (2.79)	0.037	HOMO-10→LUMO+1	28%	¹ MLCT/ ¹ LLCT/ ¹ MC	423
			HOMO-10→LUMO+3	14%	¹ MLCT/ ¹ LLCT/ ¹ MC	
			HOMO-9→LUMO+1	13%	¹ MLCT/ ¹ LLCT/ ¹ MC	

HOMO-9→LUMO+3	8%	$^1\text{MLCT}/^1\text{LLCT}/^1\text{MC}$
HOMO-10→LUMO+2	7%	$^1\text{MLCT}/^1\text{LLCT}/^1\text{MC}$

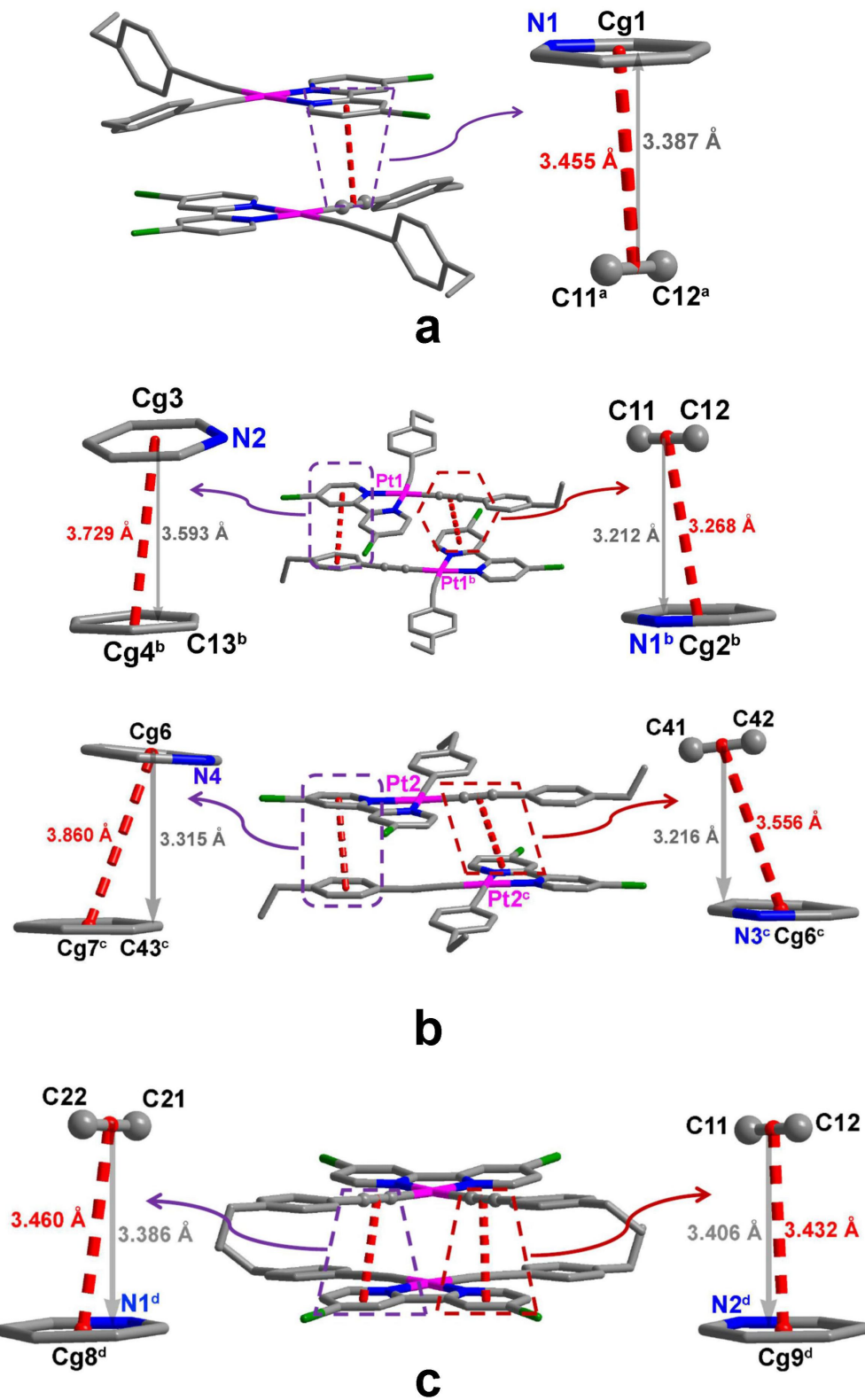


Figure S1. The π - π stacking interactions within the quasi-dimeric structure of **1**·DMSO (a) and dimeric structure of **1**·1/2(CH₃CN) (b), and one dimeric unit showing the π - π stacking interactions in the 1-D linear chain of **1**·1/8(CH₂Cl₂) (c). The hydrogen atoms are omitted for clarity. Symmetry code: a. 2-x, 1-y, 2-z; b. 1-x, -y, -z; c. 1-x, 1-y, 1-z; d. -x, 1-y, 1-z.

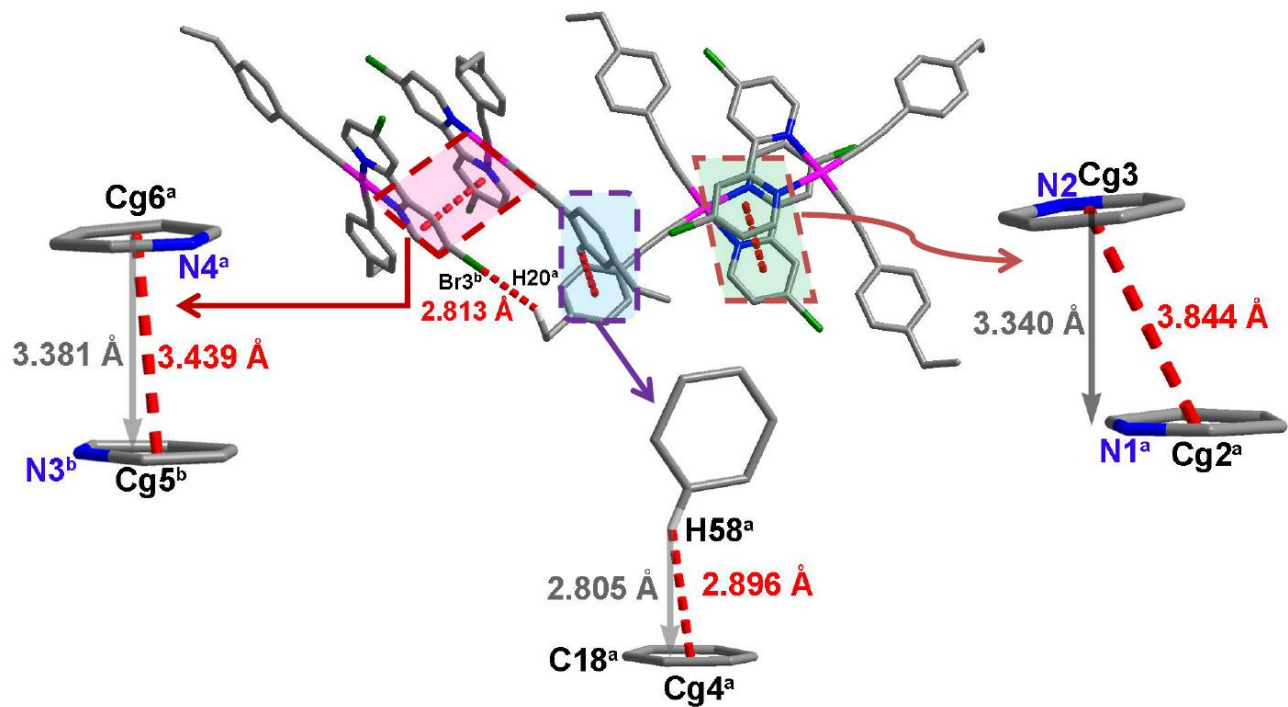


Figure S2. The interactions between adjacent dimeric structures in complex **1·1/2(CH₃CN)**. The hydrogen atoms not participate in hydrogen bond are omitted for clarity. Symmetry code: a. -x, -y, -z; b. -2+x, -1+y, -1+z.

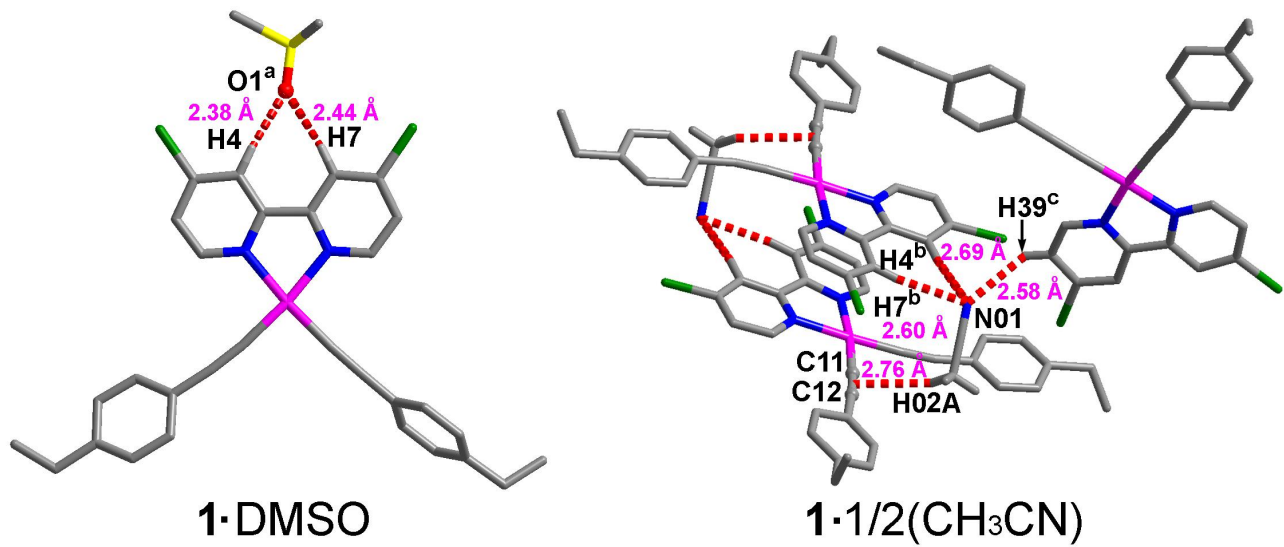


Figure S3. The hydrogen bonds between solvate molecules and Pt(II) moieties in complex **1·DMSO** and **1·1/2(CH₃CN)**. The hydrogen atoms not important are omitted for clarity. Symmetry code: a. x, y, 1+z; b. -x, -y, -z; c. -1+x, y, z.

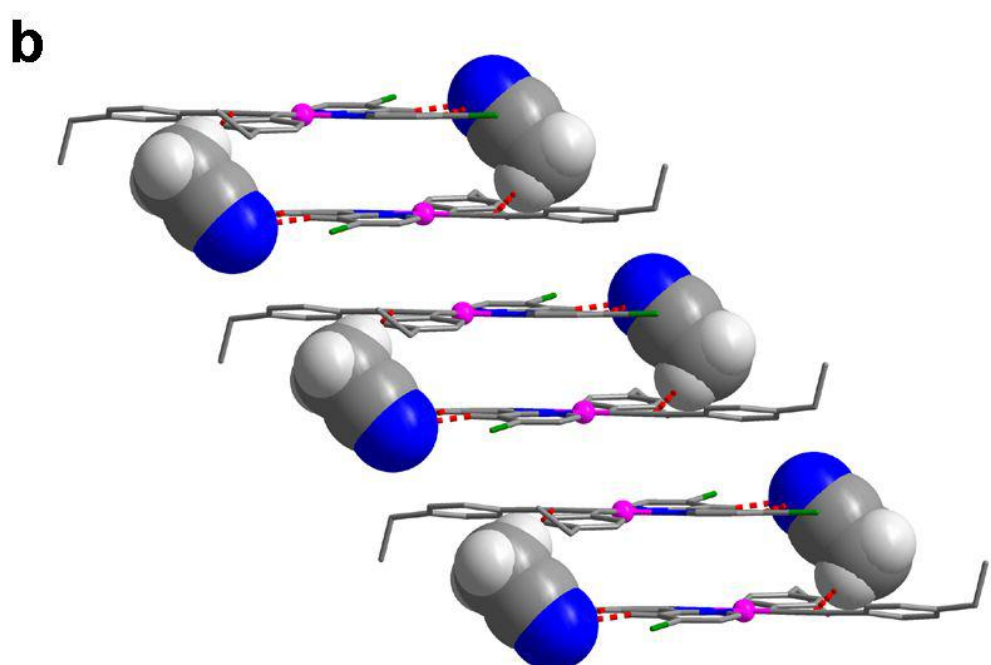
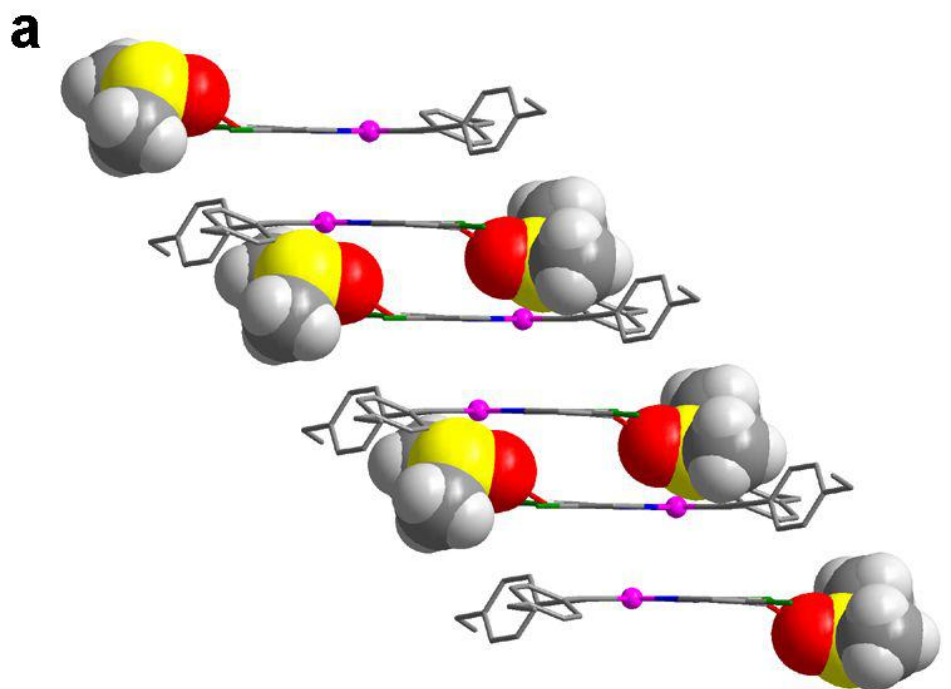


Figure S4. Packing diagrams of **1·DMSO** (a) and **1·1/2(CH₃CN)** (b), showing the Pt(II) moieties are well separated by the solvent molecules in the two phases.

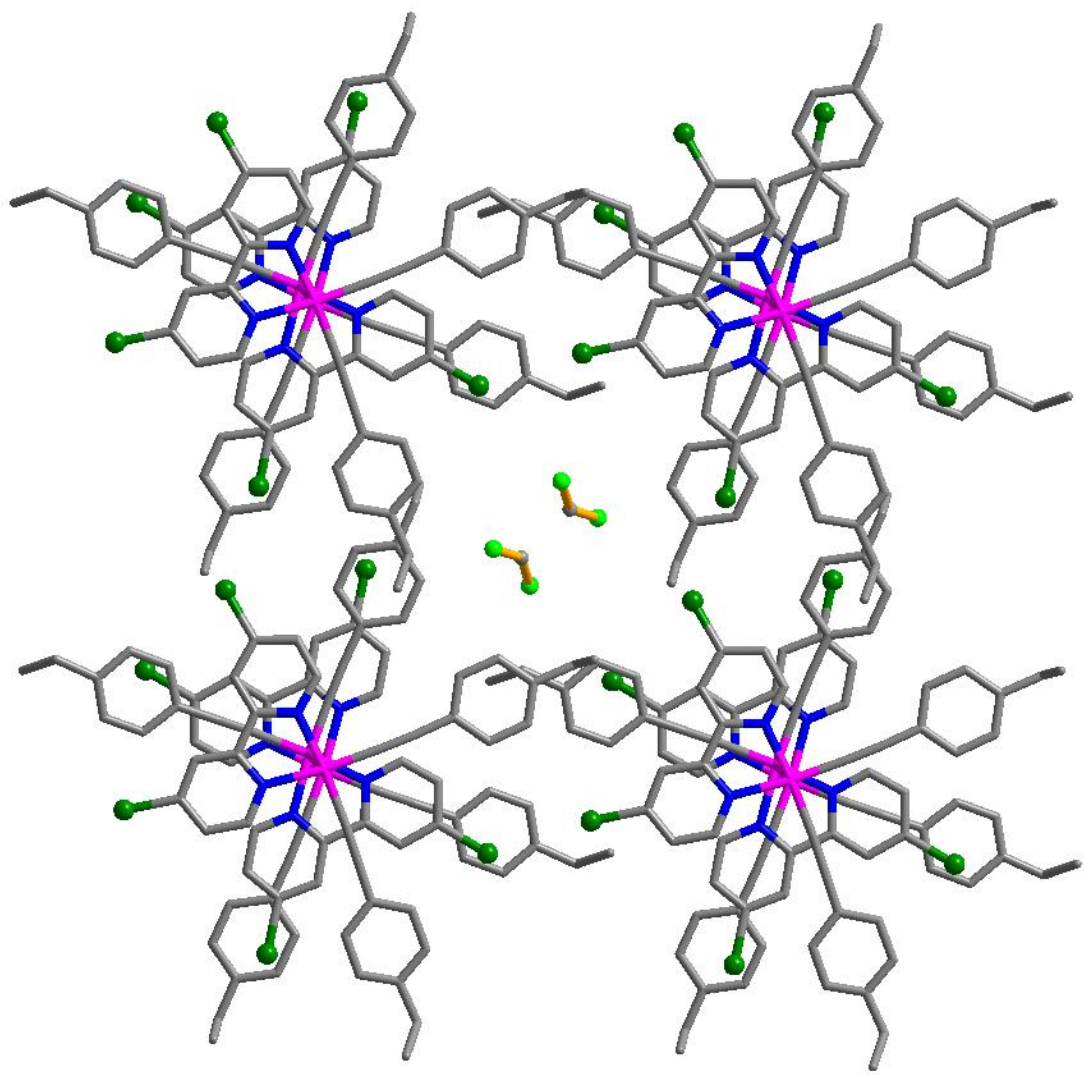


Figure S5. The stacking diagram of **1**·1/8(CH₂Cl₂), showing the CH₂Cl₂ solvate molecules located in space of crystal lattice.

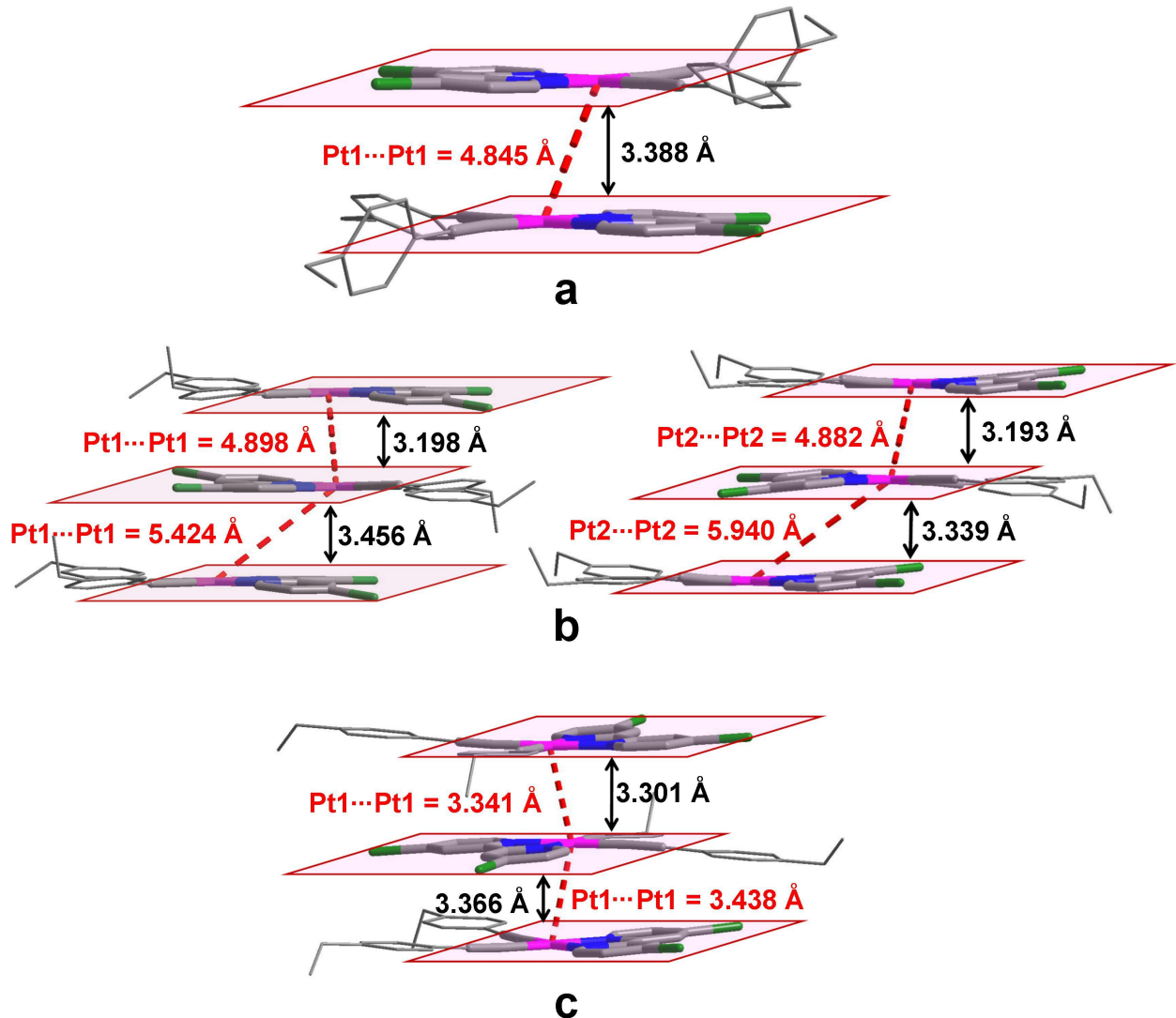


Figure S6. The Pt···Pt distances and interplanar distances in the stacking structures of **1**·DMSO (a), **1**·1/2(CH₃CN) (b), and **1**·1/8(CH₂Cl₂) (c).

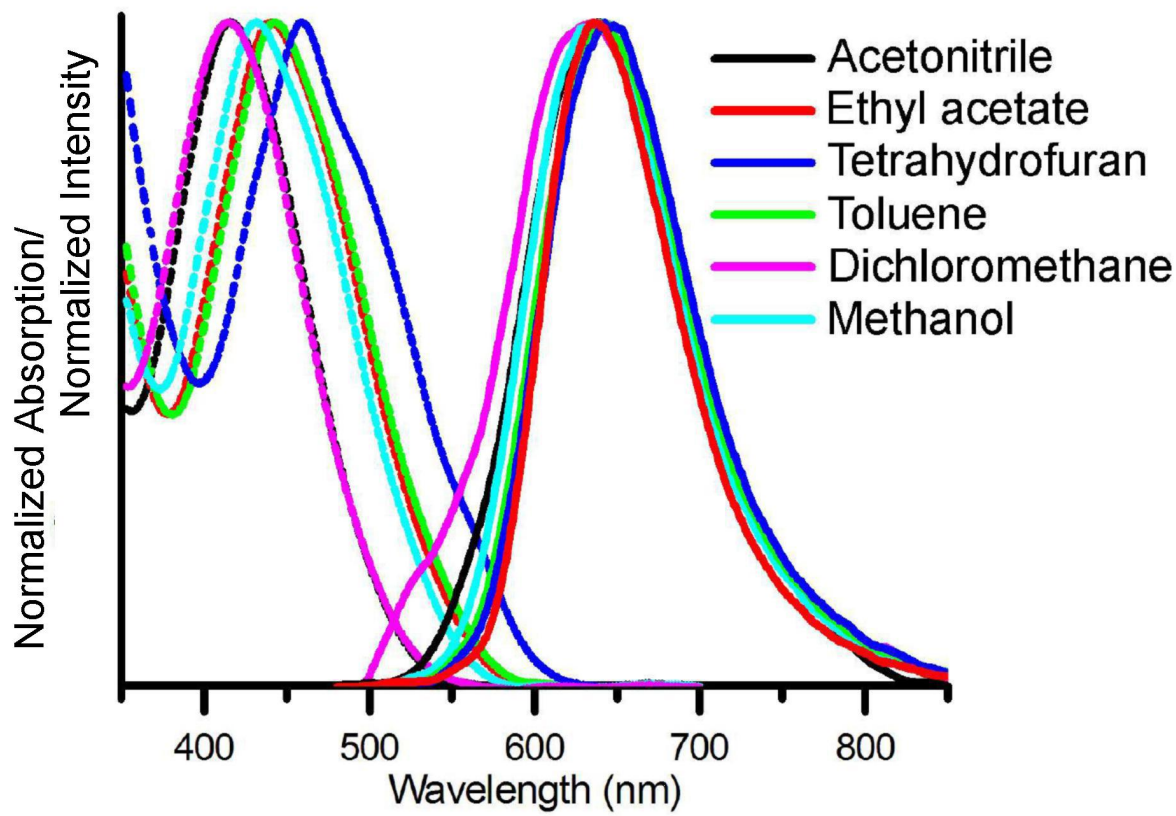


Figure S7. Low-energy absorption (dash lines) and emission spectra (solid lines) of **1** in various solvents at ambient temperature.

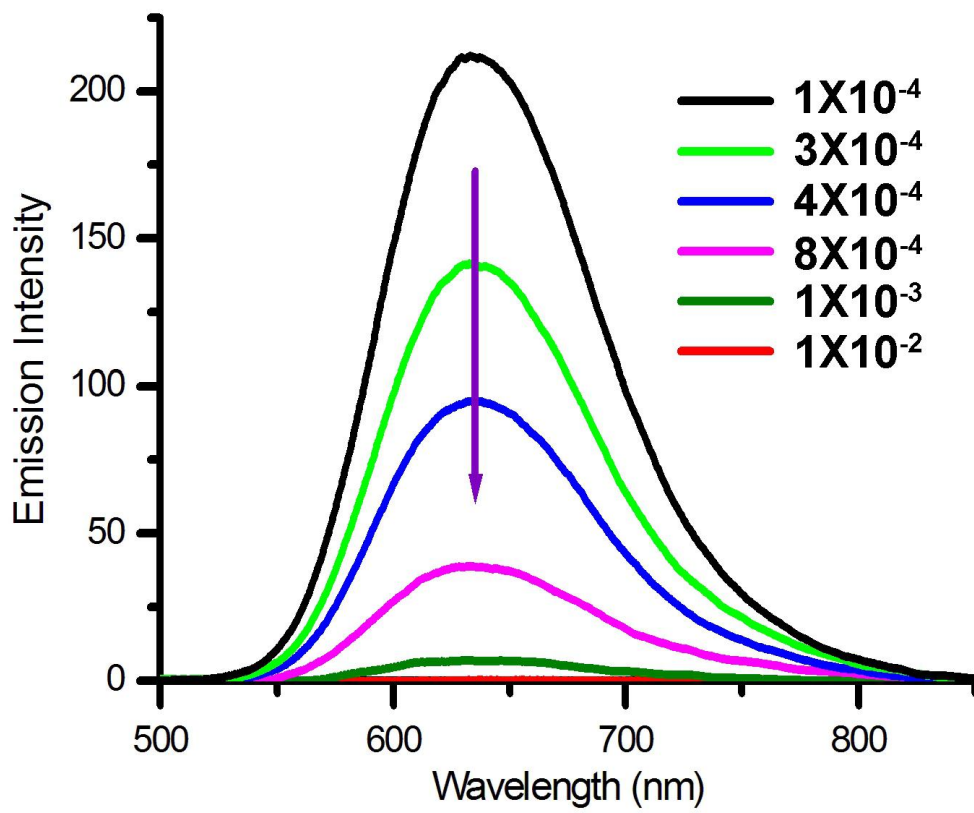


Figure S8. Emission spectra of **1** in dichloromethane solution with different concentration.

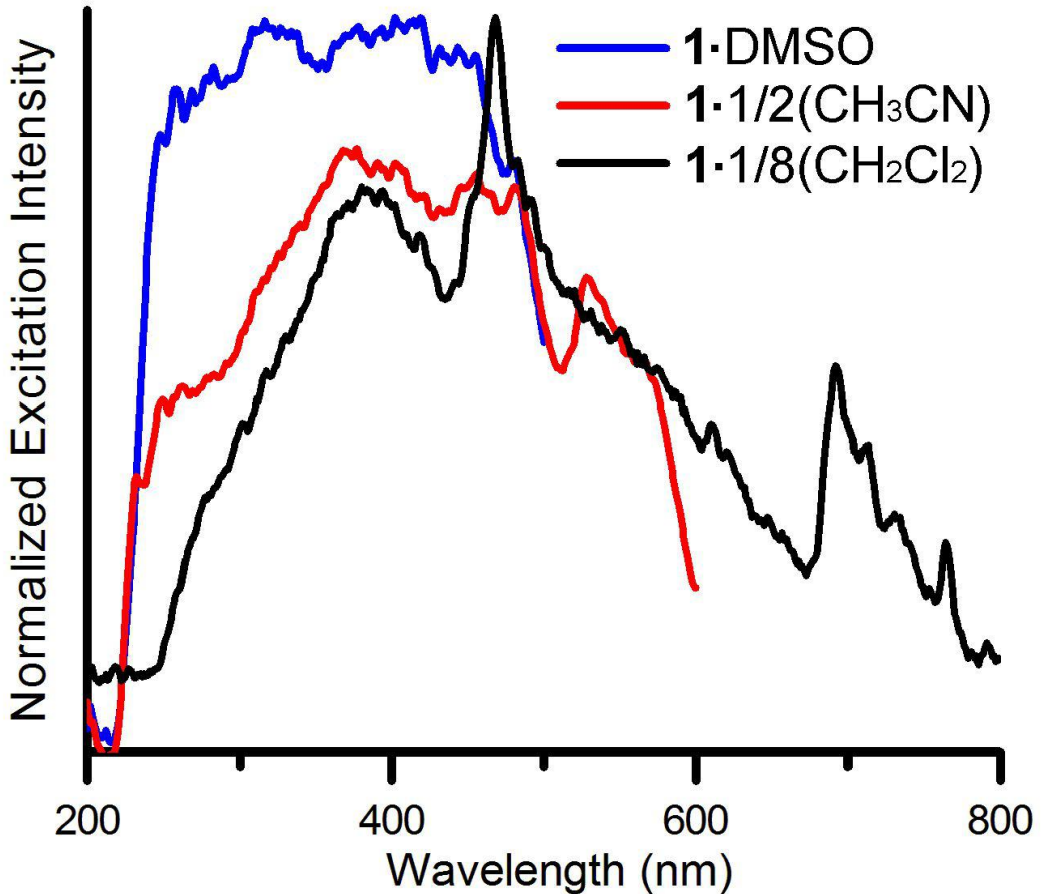


Figure S9. The excitation spectra of solid samples **1·DMSO**, **1·1/2(CH₃CN)**, and **1·1/8(CH₂Cl₂)** at ambient temperature.

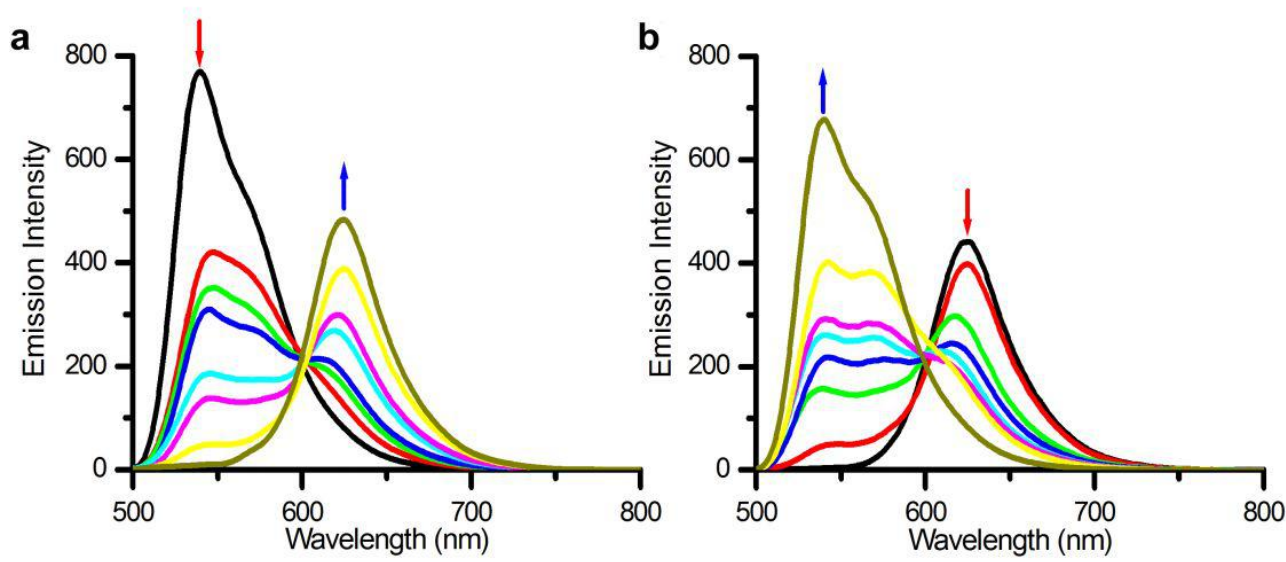


Figure S10. Emission spectral changes of solid **1**·DMSO in response to CH_3CN vapor (left) and $1 \cdot 1/2(\text{CH}_3\text{CN})$ to DMSO vapor (right), showing gradual interconversions between two vibronic-structured emission bands (540 and 570 nm) and a broad unstructured emission band (625 nm).

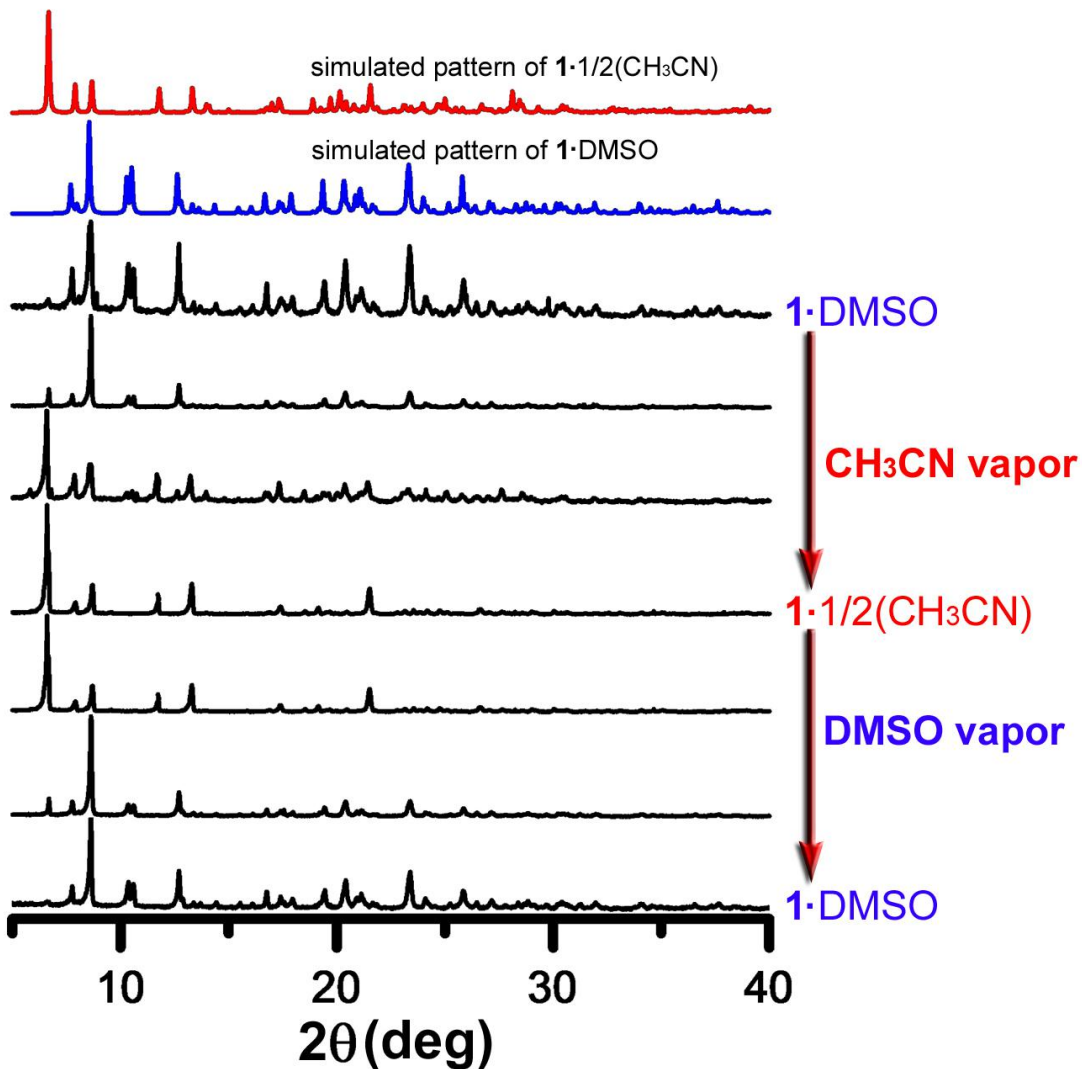


Figure S11. The XRD diagrams recorded in a reversible vapochromic cycle **1·DMSO**↔**1·1/2(CH₃CN)**, showing dynamic variations of XRD patterns from **1·DMSO**→**1·1/2(CH₃CN)** upon exposure of **1·DMSO** into a saturated CH₃CN vapor, and the XRD patterns from **1·1/2(CH₃CN)**→**1·DMSO** by exposing **1·1/2(CH₃CN)** into DMSO vapor at ambient temperature.

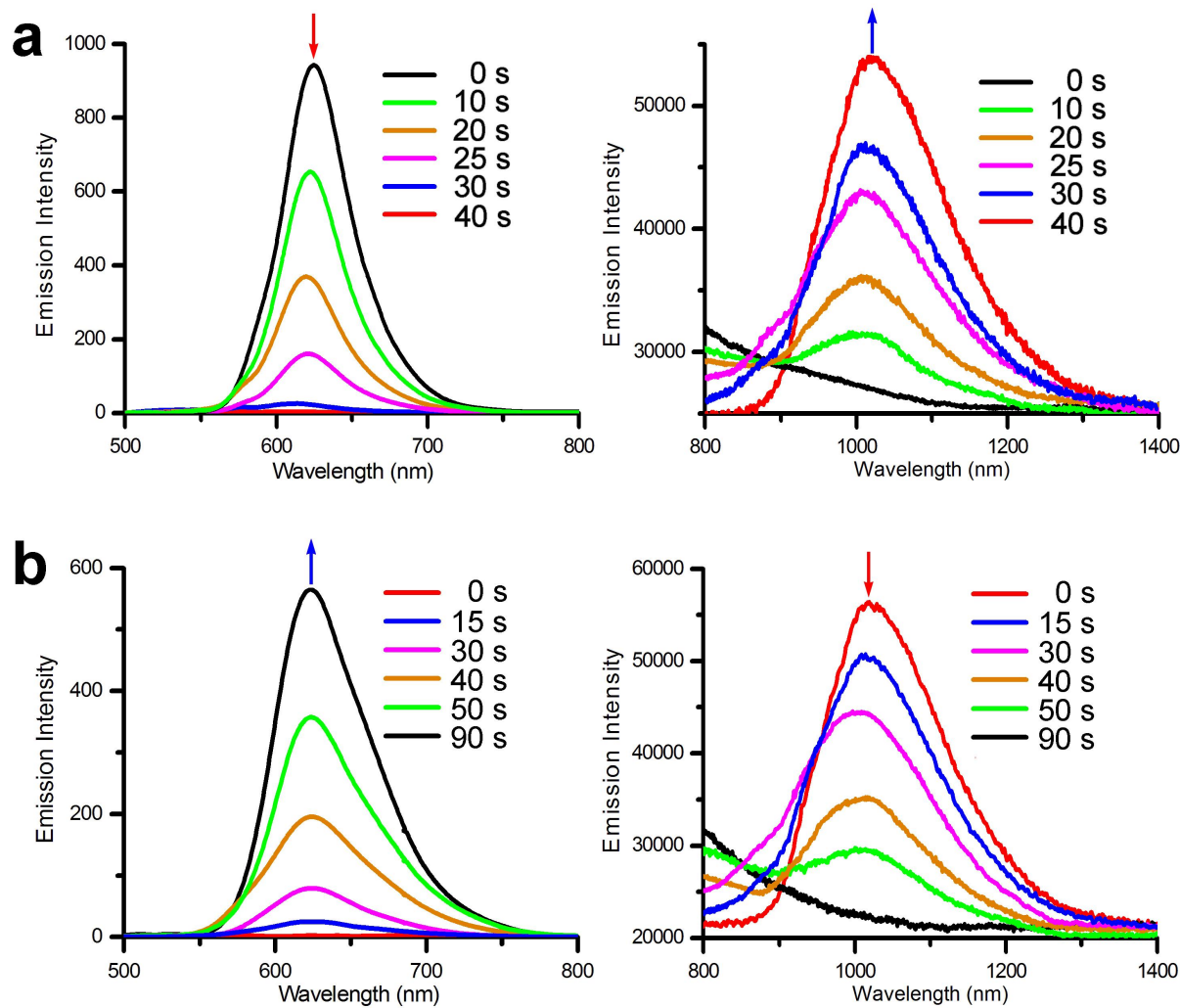


Figure S12. Emission spectral changes (left is in visible region and right is in NIR region) of solid **1·1/2(CH₃CN)** sample in response to CH₂Cl₂ vapor (a) and **1·1/8(CH₂Cl₂)** in response to CH₃CN vapor (b), showing gradual interconversions between emission bands in visible region (625 nm) and in NIR region (1022 nm).

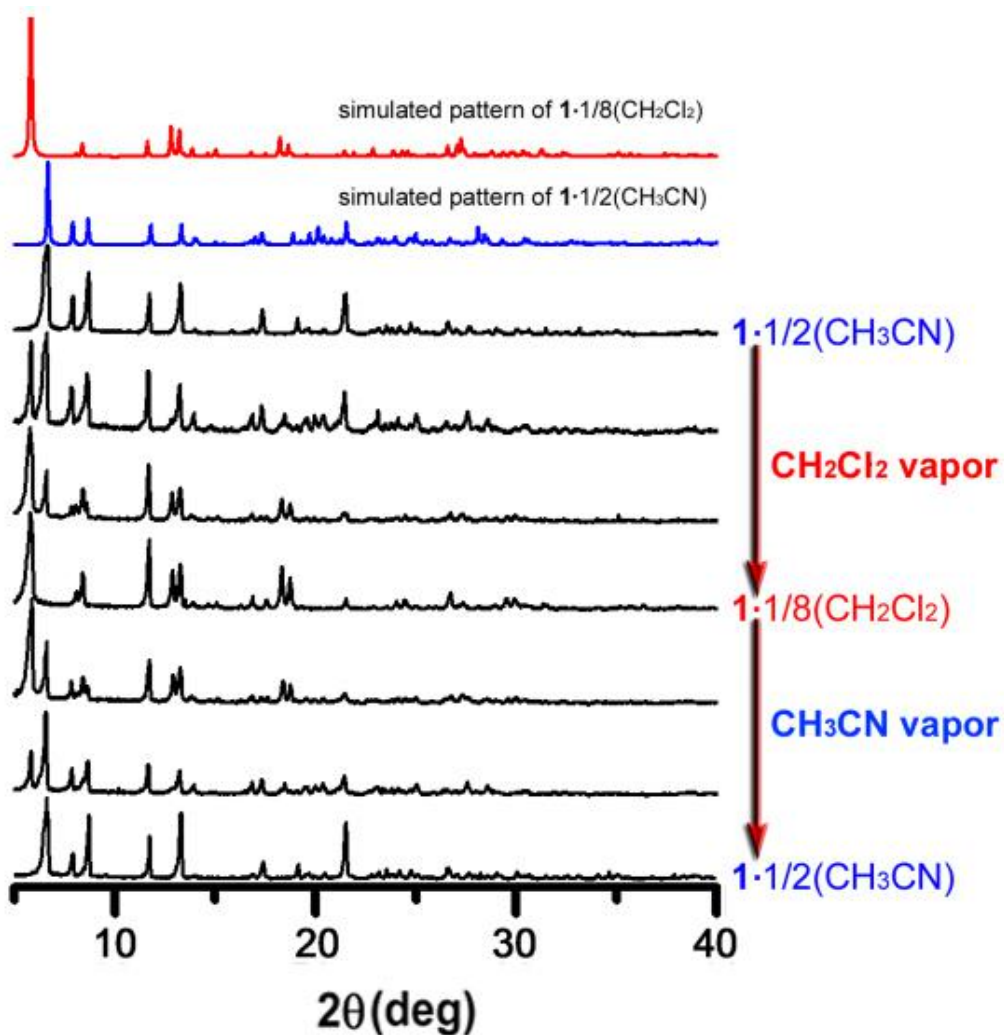


Figure S13. The XRD diagrams recorded in a reversible vapochromic cycle $1 \cdot 1/2(\text{CH}_3\text{CN}) \rightleftharpoons 1 \cdot 1/8(\text{CH}_2\text{Cl}_2)$, showing dynamic variations of XRD patterns from $1 \cdot 1/2(\text{CH}_3\text{CN}) \rightarrow 1 \cdot 1/8(\text{CH}_2\text{Cl}_2)$ upon exposure of $1 \cdot 1/2(\text{CH}_3\text{CN})$ into a saturated CH_2Cl_2 vapor, and the XRD patterns from $1 \cdot 1/8(\text{CH}_2\text{Cl}_2) \rightarrow 1 \cdot 1/2(\text{CH}_3\text{CN})$ by exposing $1 \cdot 1/8(\text{CH}_2\text{Cl}_2)$ into CH_3CN vapor at ambient temperature.

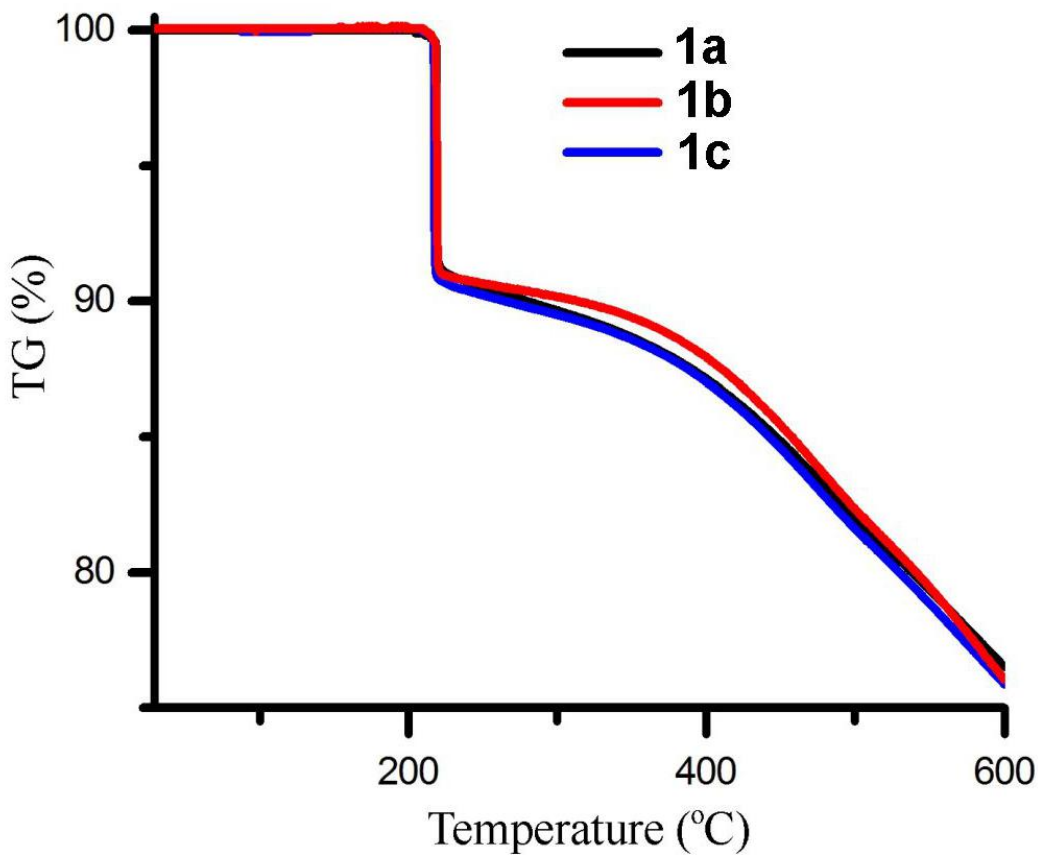
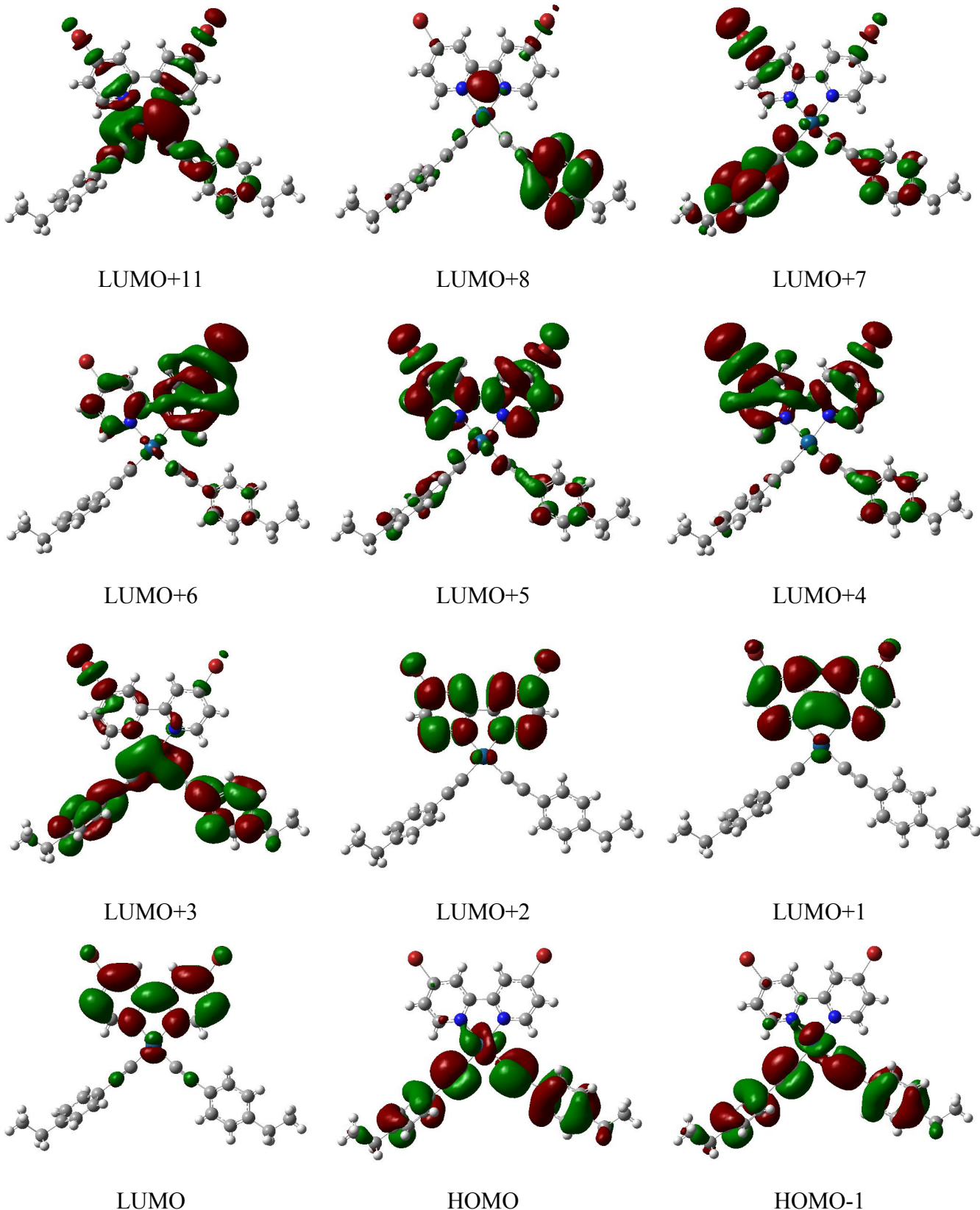


Figure S14. Thermogravimetric analysis curves of the three heated samples **1a**, **1b** and **1c**.



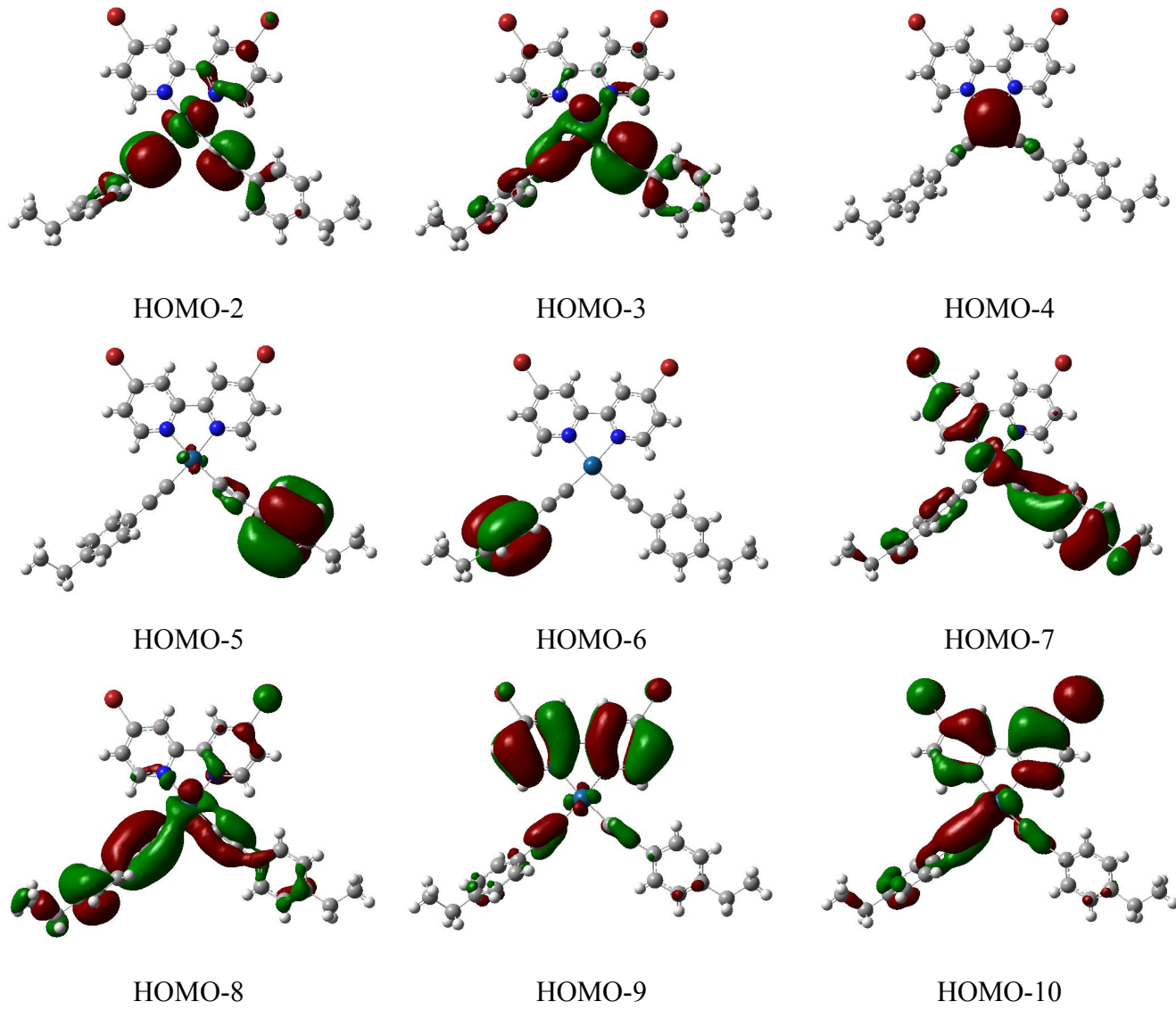
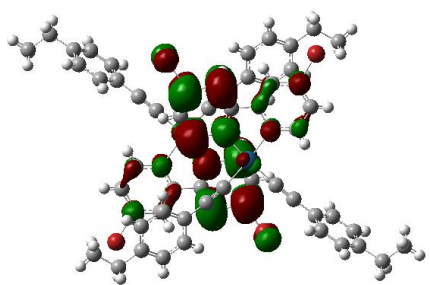
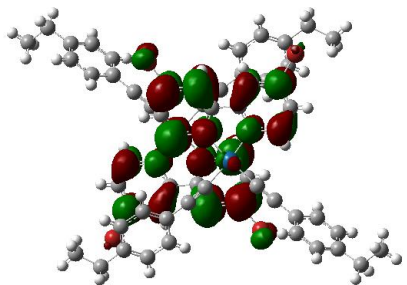


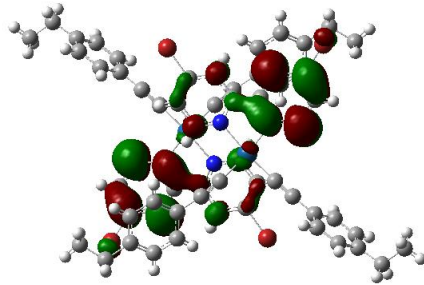
Figure S15. Plots of the frontier molecular orbitals involved in the absorption transition for complex **1** in dichloromethane solution (isovalue = 0.02).



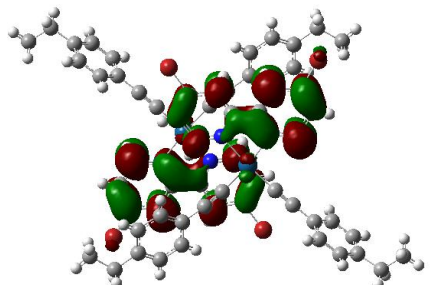
LUMO+5



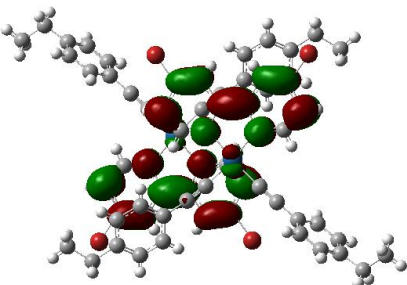
LUMO+4



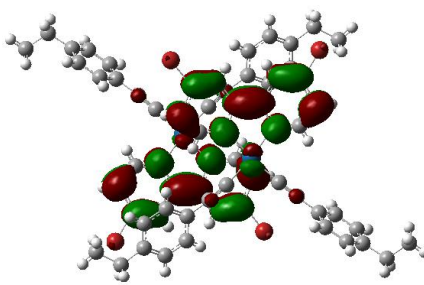
LUMO+3



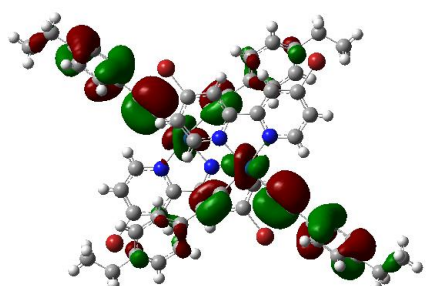
LUMO+2



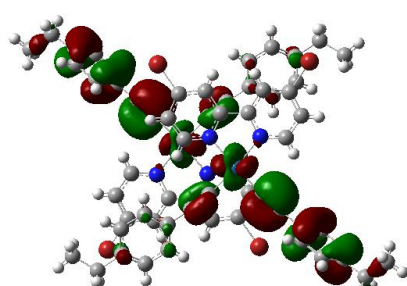
LUMO+1



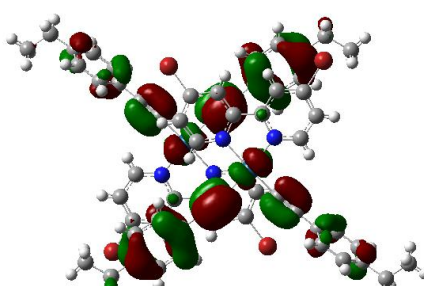
LUMO



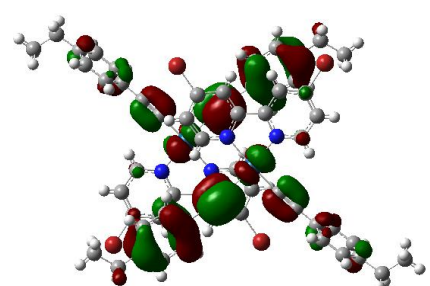
HOMO



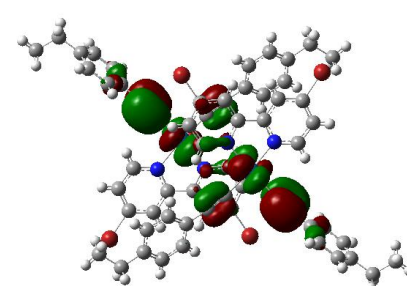
HOMO-1



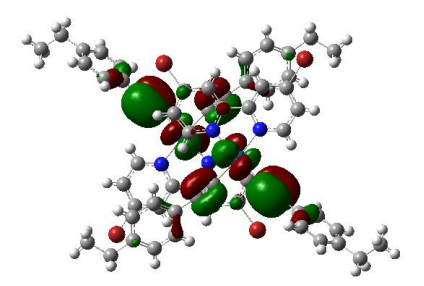
HOMO-2



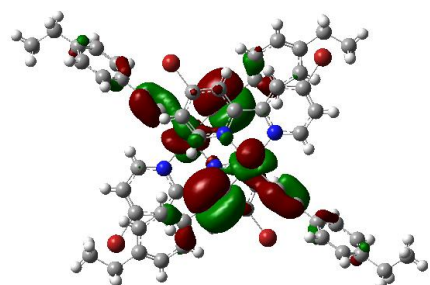
HOMO-3



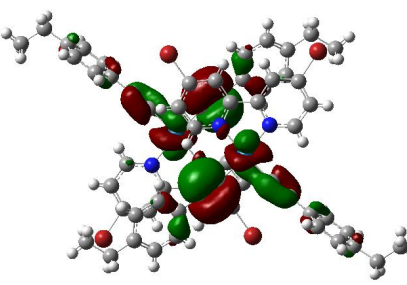
HOMO-4



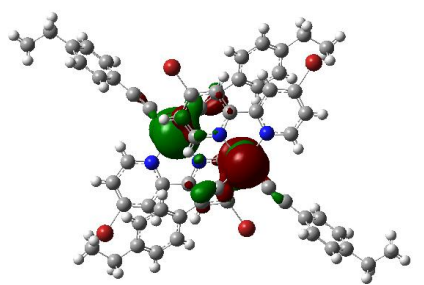
HOMO-5



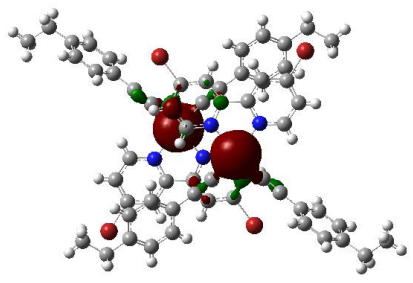
HOMO-6



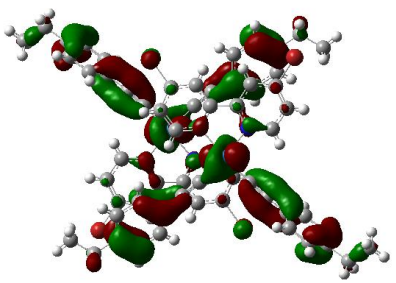
HOMO-7



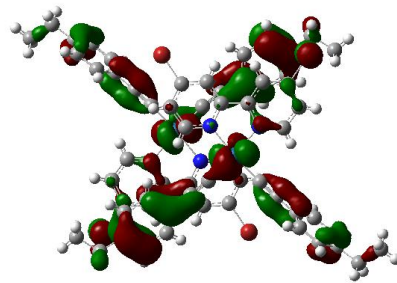
HOMO-8



HOMO-9

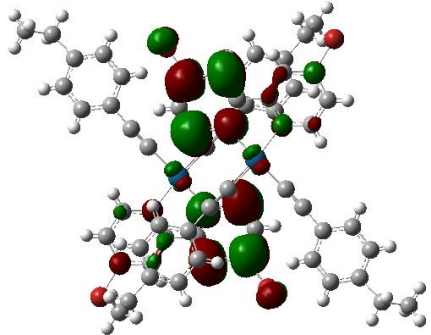


HOMO-14

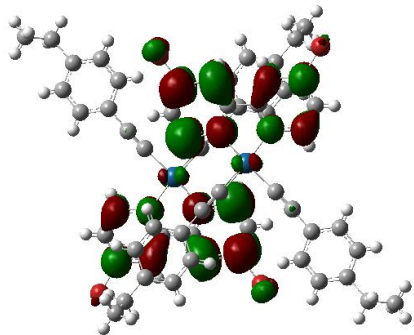


HOMO-15

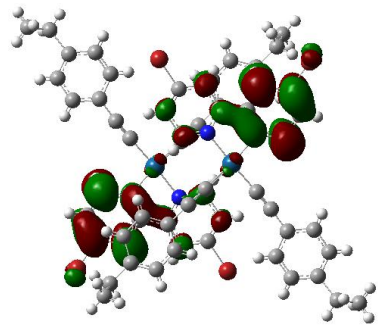
Figure S16. Plots of the frontier molecular orbitals involved in the absorption transition for the two-molecule model of **1**·DMSO (isovalue = 0.02).



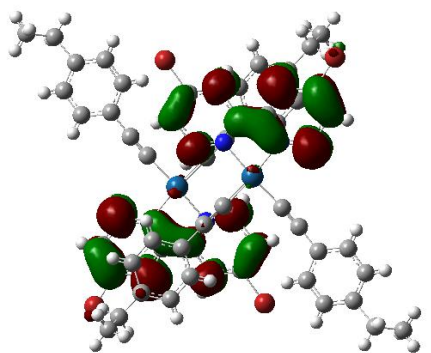
LUMO+5



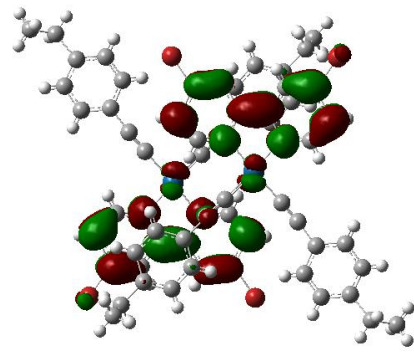
LUMO+4



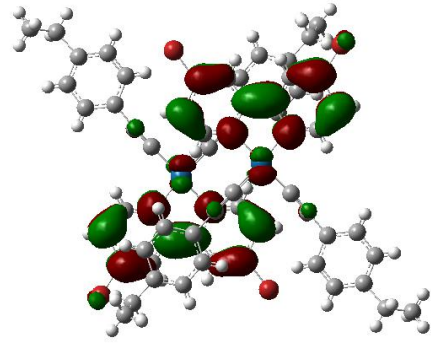
LUMO+3



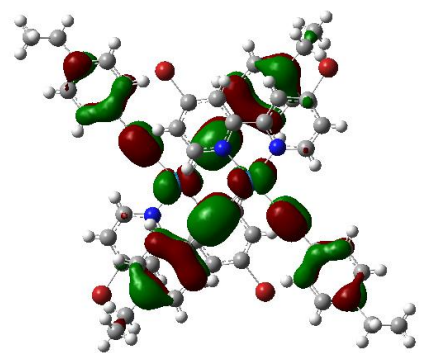
LUMO+2



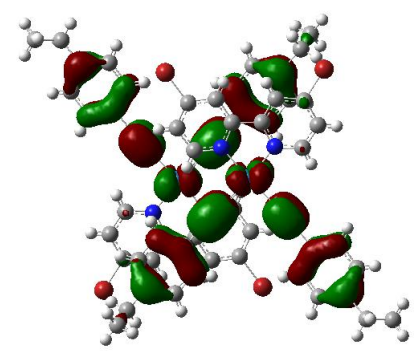
LUMO+1



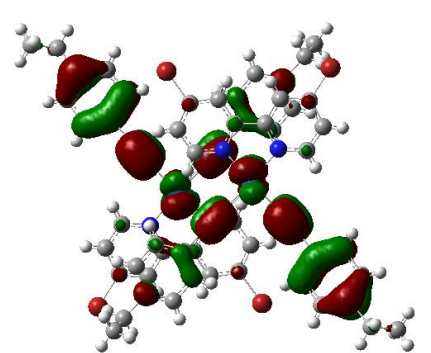
LUMO



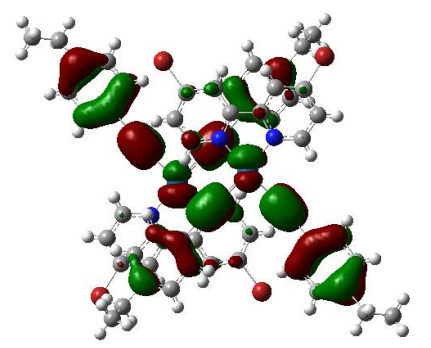
HOMO



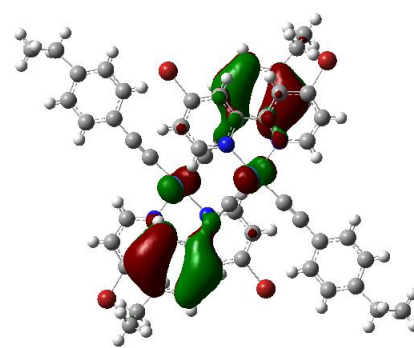
HOMO-1



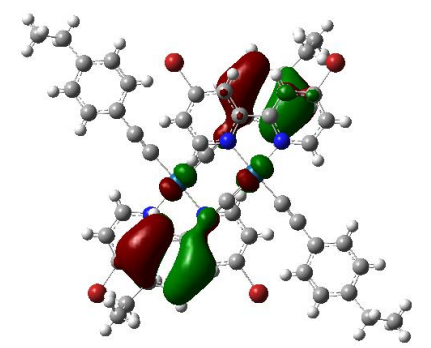
HOMO-2



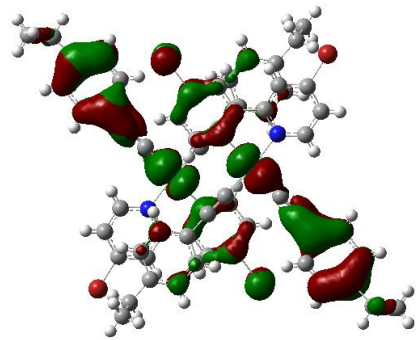
HOMO-3



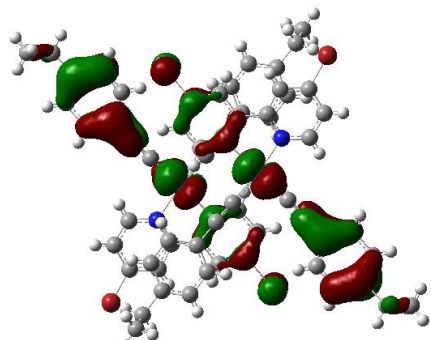
HOMO-12



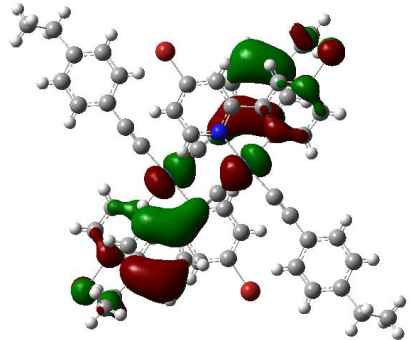
HOMO-13



HOMO-14

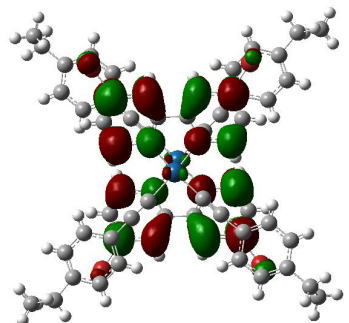


HOMO-15

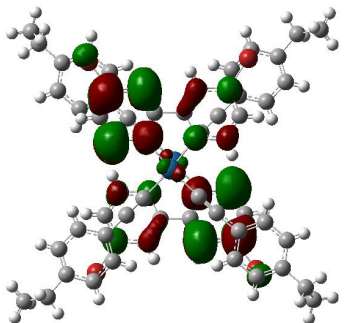


HOMO-16

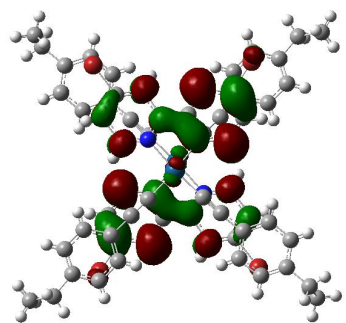
Figure S17. Plots of the frontier molecular orbitals involved in the absorption transition for the two-molecule model of **1·1/2(CH₃CN)** (isovalue = 0.02).



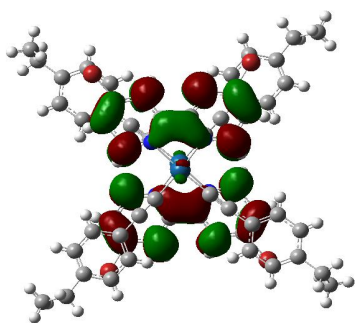
LUMO+5



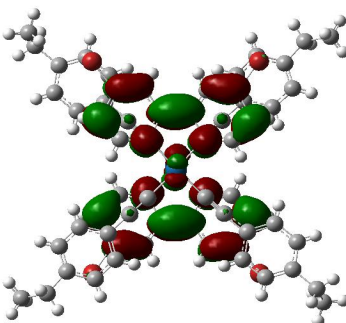
LUMO+4



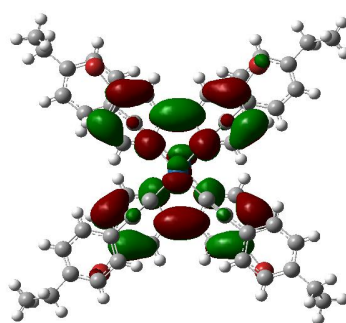
LUMO+3



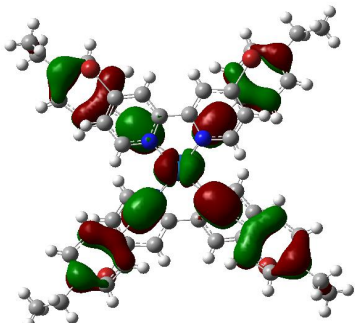
LUMO+2



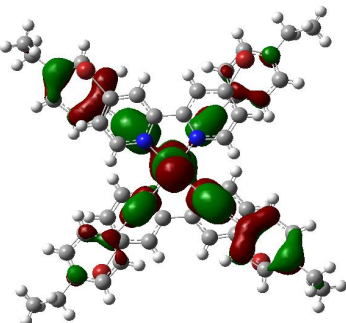
LUMO+1



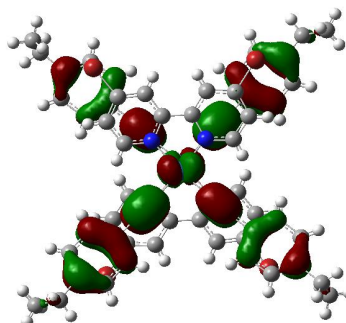
LUMO



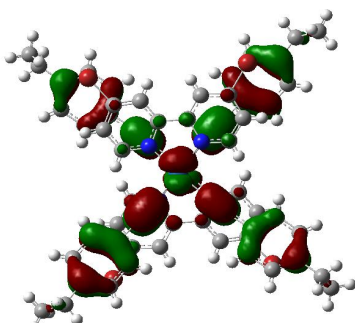
HOMO



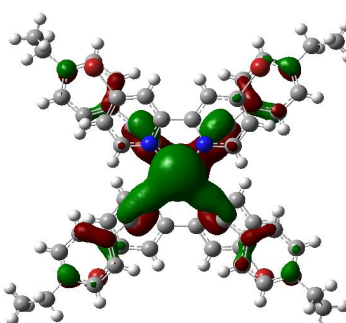
HOMO-1



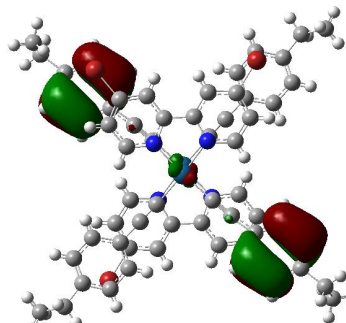
HOMO-2



HOMO-3



HOMO-4



HOMO-9

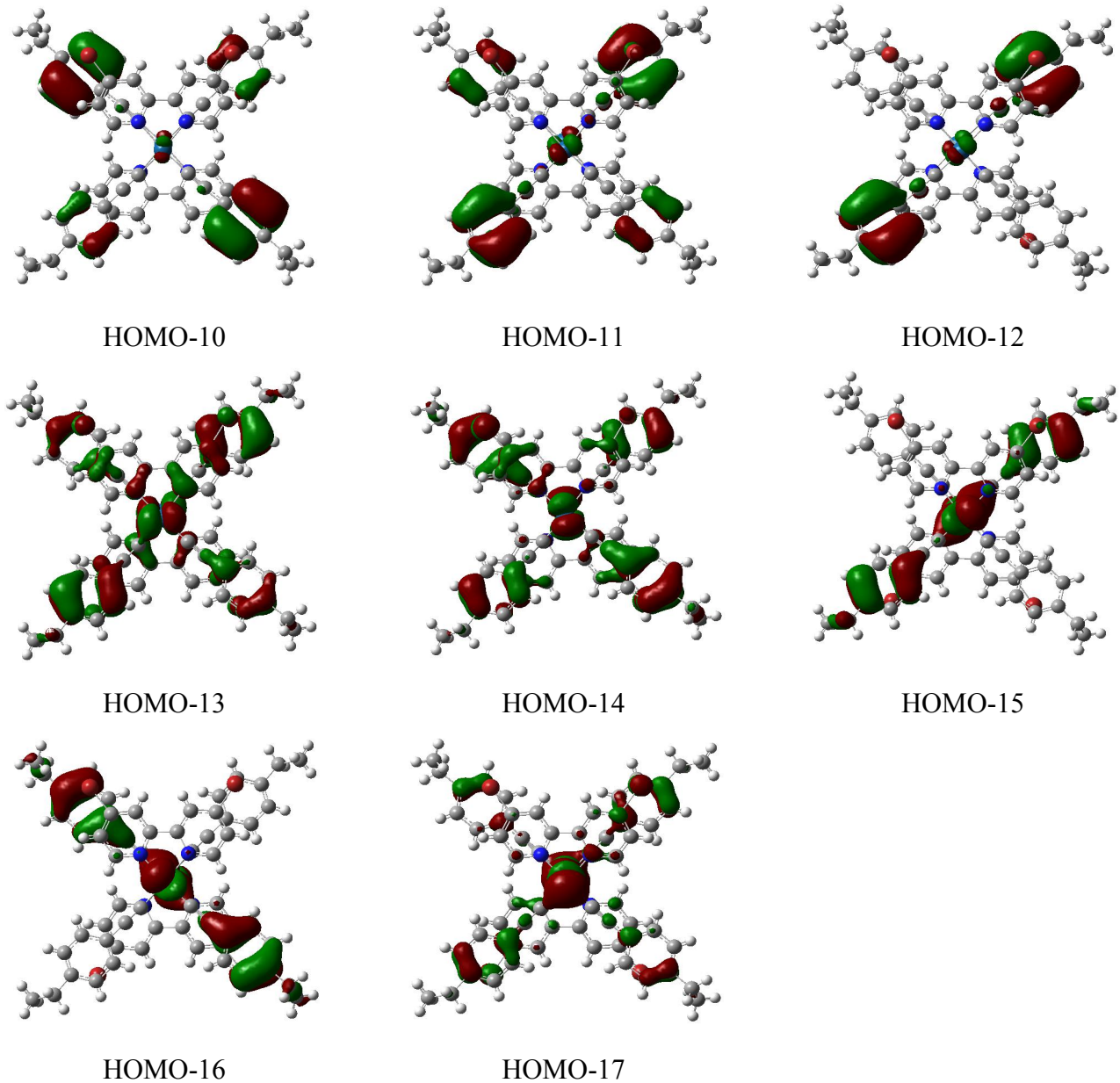
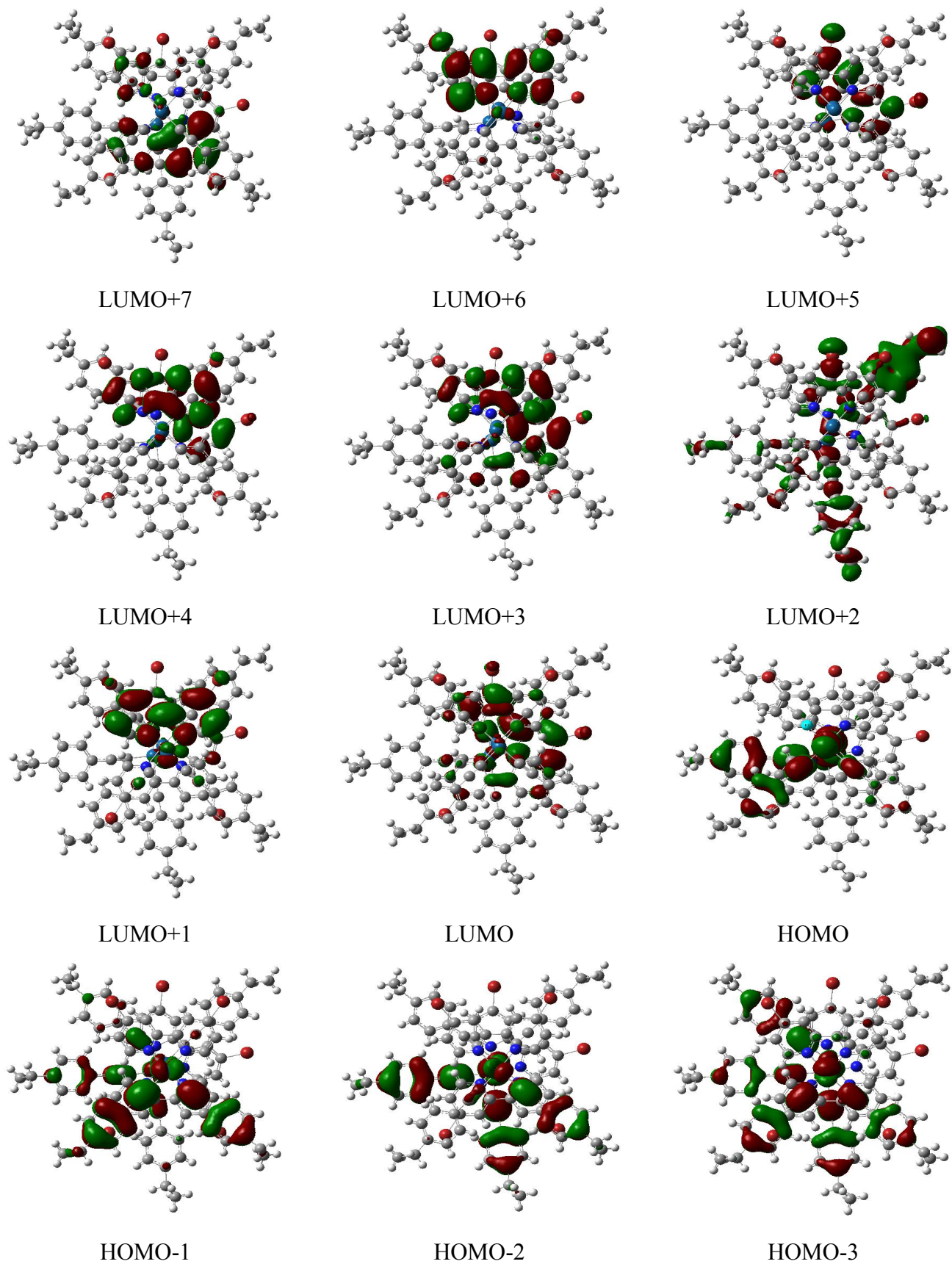


Figure S18. Plots of the frontier molecular orbitals involved in the absorption transition for two-molecule model of **1**·1/8(CH₂Cl₂) (isovalue = 0.02).



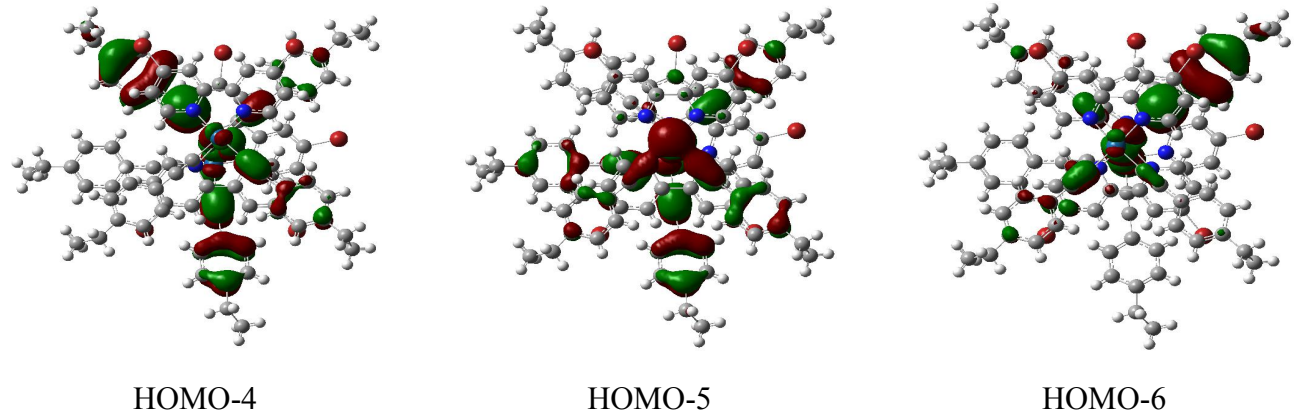
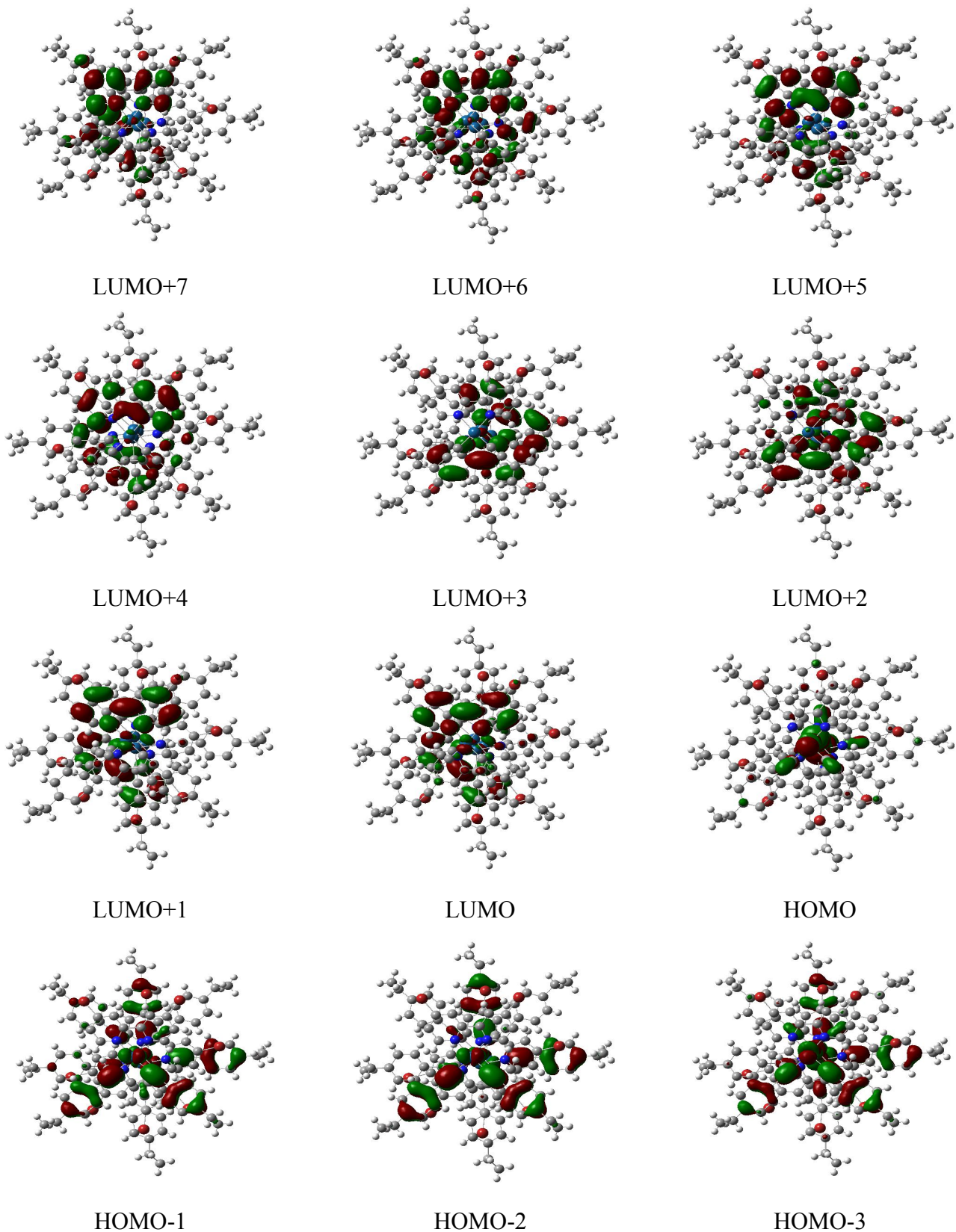


Figure S19. Plots of the frontier molecular orbitals involved in the absorption transition for three-molecule model of **1**·1/8(CH₂Cl₂) (isovalue = 0.02).



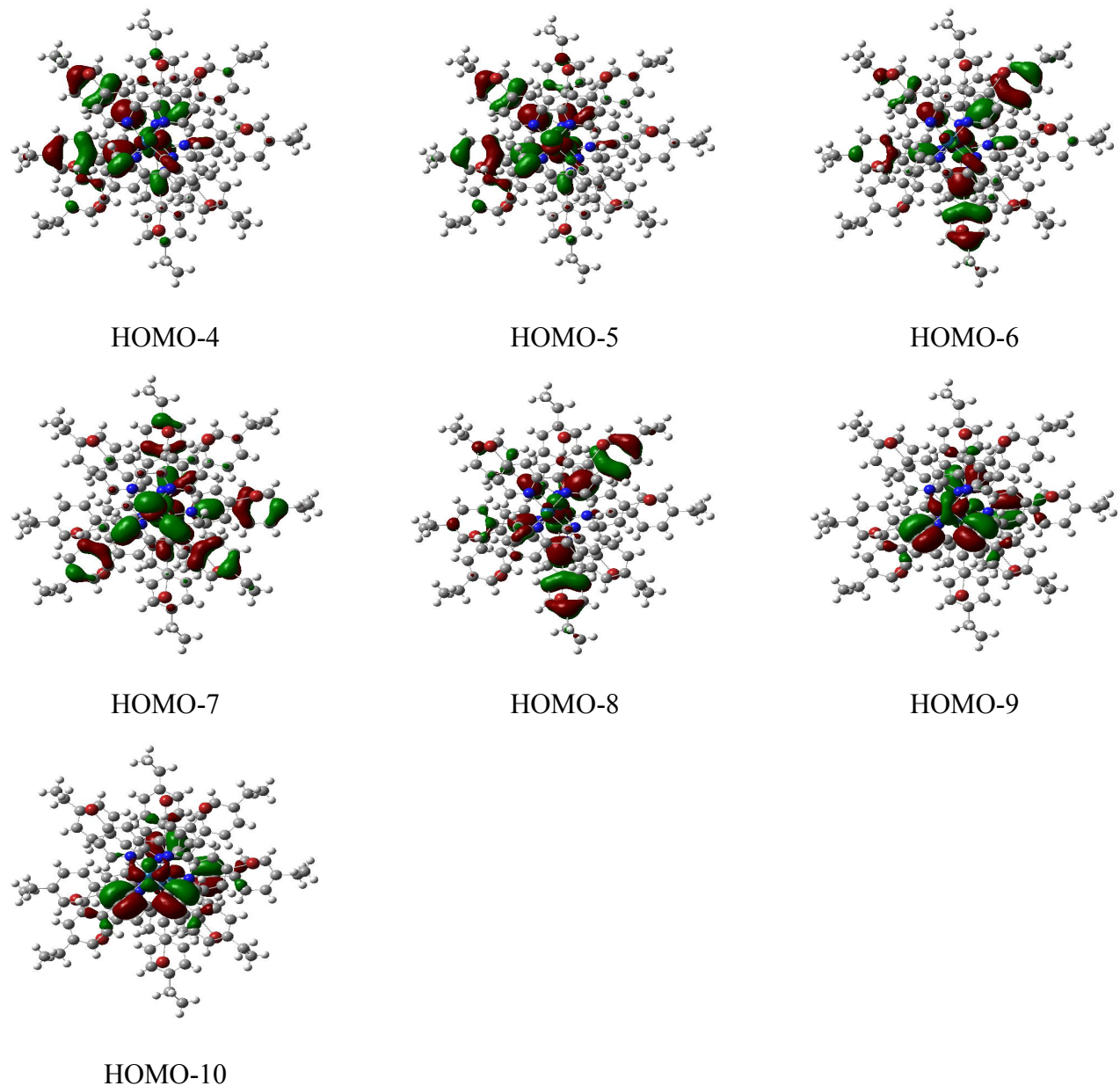
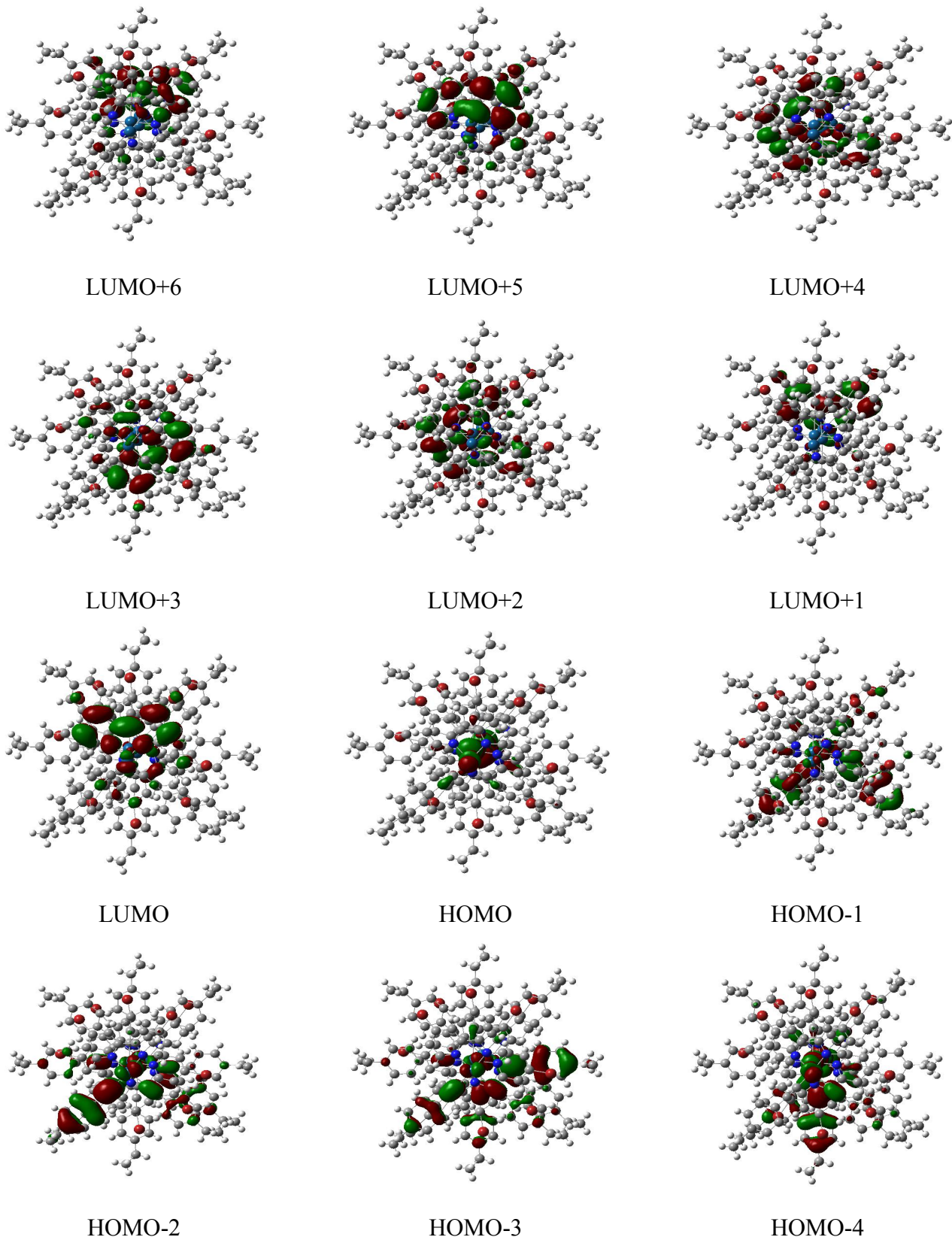


Figure S20. Plots of the frontier molecular orbitals involved in the absorption transition for four-molecule model of $\mathbf{1} \cdot \frac{1}{8}(\text{CH}_2\text{Cl}_2)$ (isovalue = 0.02).



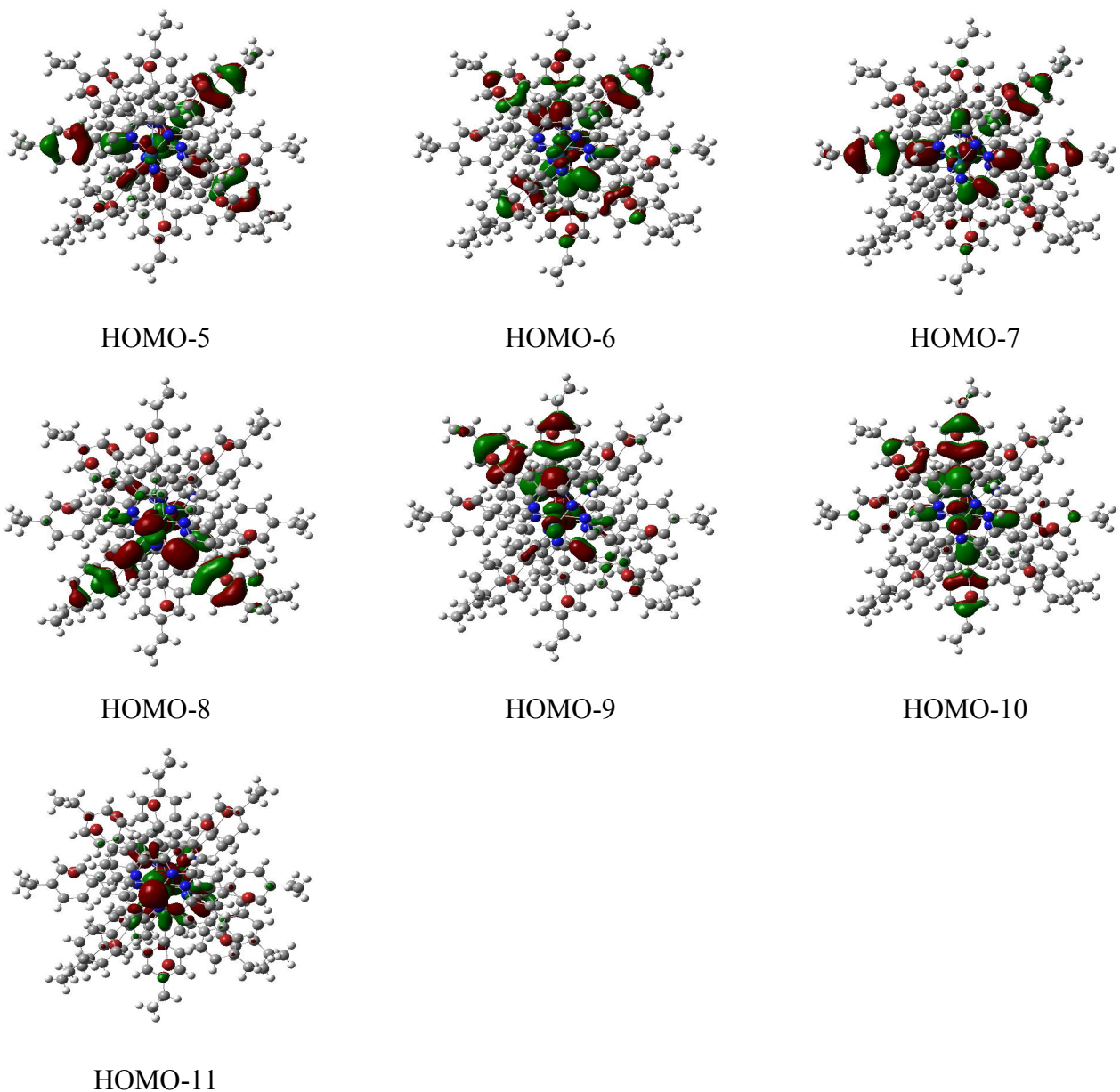


Figure S21. Plots of the frontier molecular orbitals involved in the absorption transition for five-molecule model of **1·1/8(CH₂Cl₂)** (isovalue = 0.02).